Computational Overview of a Pd-Catalyzed Olefin Bis-alkoxycarbonylation Process

(Article begins on next page)

18 September 2024

A Computational Overview of a Pd-Catalyzed Olefin bis-Alkoxycarbonylation Process

Carlo Mealli,[†] Gabriele Manca,*,[†] Riccardo Tarroni,[‡] Diego Olivieri[‡] and Carla Carfagna[‡]
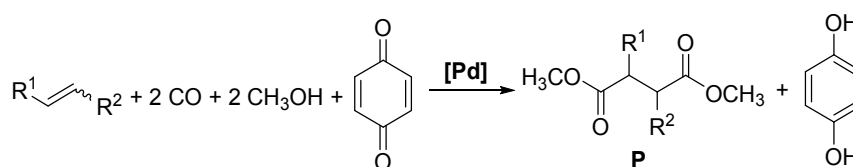
[†] Istituto di Chimica dei Composti OrganoMetallici, CNR-ICCOM, Via Madonna del Piano 10, I-50019 Sesto Fiorentino, Florence (FI), Italy.

[‡]Department of Industrial Chemistry "T. Montanari", University of Bologna, Viale Risorgimento 4, 40136 Bologna (BO), Italy.

ABSTRACT: A comprehensive DFT analysis is reported for the one pot bis-alkoxycarbonylation reaction of olefins, which affords succinic acid esters by action of the catalyst (N-N)Pd(TFA)$_2$ (N-N = bis-(2,6-dimethylphenyl)-2,3-dimethyl-1,4-diazabutadiene, TFA$^-$ = CF$_3$CO$_2$$^-$). The selective and efficient process involves alkene (H$_2$C=CHR), CO, methanol and *p*-benzoquinone (BQ) molecules as reactants. The catalytic mechanism, previously proposed on the basis of available experimental and literature data, is here critically revised by the *in silico* analysis. A plethora of optimized intermediates and transition states and their correlating energy profiles allows a step by step reconstruction of the entire cycle, shading light on key mechanistic aspects, such as for instance the role of the R substituent in the olefin. One of its effects is determined by the presence of a 2e$^-$ donor group, which, depending on its power, may affect the catalysis up to its total inhibition. As another aspect, the key diester product forms through a reductive elimination step (Pd(II)➔Pd(0) transformation), that excludes the previously proposed attainment of a Pd(II)-hydride complex. Finally, the paper illustrates the action of the sacrificial BQ oxidant in the restoration of the original Pd(II) catalyst, as found for other strictly related cases. The energy profile indicates that the rate determining step occurs in the initial part of the reaction, given a +29.7 kcal mol^{-1} energy barrier, associated with a methoxo migration into an adjacent CO ligand. The result foreshadows a rather slow activation of the catalyst and a long duration of the cycle.
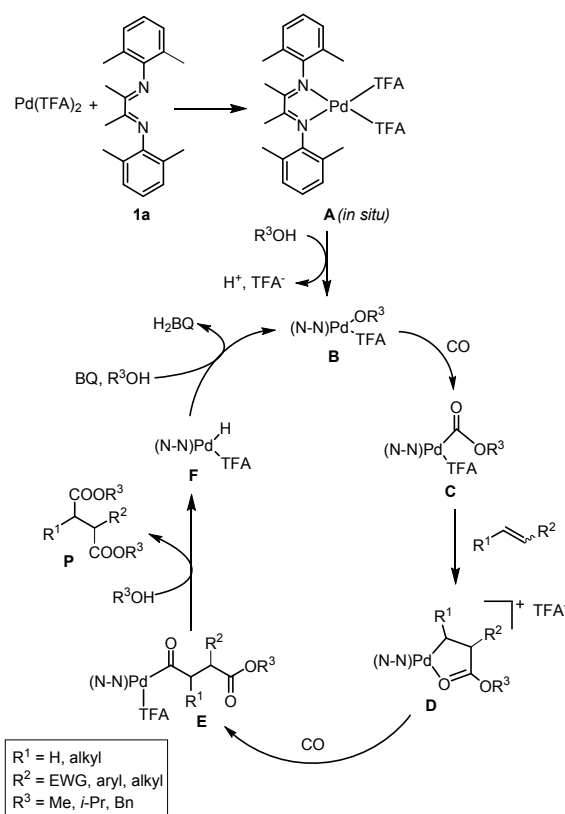
Introduction

Carbonylations are among the most important reactions in organometallic and organic chemistry for converting inexpensive feedstock such as alkenes or alkynes and CO into highly valuable carbonylated compounds.[1] In particular, in the bis-alkoxycarbonylation of olefins a double addition of an alkoxycarbonyl group occurs with the formation of succinic acid ester derivatives (Scheme 1). These are important building blocks in both organic and medicinal chemistry,[2] to be used in many industrial fields.[3]

Scheme 1. Pd-catalyzed bis-alkoxycarbonylation reaction of alkenes involving carbon monoxide, methanol and *p*-benzoquinone.

Some of us (*C.C.* et al.) have reported a selective and efficient oxidative[4] Pd-catalyzed bis-alkoxycarbonylation processes for both terminal[5a] and 1,2-disubstituted alkenes.[5] The catalyst was formed *in situ* by mixing $Pd(TFA)_2$ and an appropriate aryl α-diimine molecule.[6] The reaction proceeds under 4 bar pressure of CO at 20°C in the MeOH/THF 7:1 reaction medium, employing *p*-benzoquinone (BQ) as a sacrificial oxidant, which transforms into 1,4-hydroquinone (H_2BQ). Additionally, the process is favoured in an acidic environment by adding for instance the *p*-toluenesulfonic acid (*p*-TSA). More recently, we also reported the first example of bis-alkoxycarbonylation reaction of electron-deficient olefins,[5c] employing an analogous catalytic system. High yields and complete selectivities were obtained starting from differently substituted acrylic esters and amides.

For all the studied cases, a similar catalytic cycle, such as that in Scheme 2, was proposed.[7] The pre-catalyst is the Pd(II) square planar complex (N-N)Pd(TFA)$_2$ **A**, that features the bis-nitrogen ligand **1a**, namely bis-(2,6-dimethylphenyl)-2,3-dimethyl-1,4-diazabutadiene, plus two trifluoroacetate anions (TFA$^-$).[5b] The Pd complex reacts with the alcohol allowing the formation of the active species **B**.[8] The successive insertion of CO leads to the alkoxycarbonyl-palladium complex **C**,[9] where the subsequent alkene's coordination and insertion afford the 5-membered palladacycle **D**.[10,11] From the latter, the complex **E** is obtained via another CO insertion passing through a 6-membered palladacycle with the esteric carbonyl coordinated to the Pd center.[5c]

Scheme 2. Proposed catalytic mechanism for the bis-alkoxycarbonylation of olefins catalysed by aryl α-diimine/Pd(II) complexes. EWG = Electron-Withdrawing Group.

Hence, the nucleophilic attack of another methanol molecule to the coordinated acyl group in **E** would afford the final product **P** together with the palladium hydride complex **F**.[7c] Eventually, the *p*-benzoquinone molecule, that enters the scene only after the departure of **P**, regenerates the active species.[12,13] The possible BQ role was already established by one of us (*C.M.*) for a

3

similarly behaving system,[14] which involves the reductive elimination of an allylic amine. The latter mechanism can be at work also in the release of the present **P** product**,** implying, also in this case, the formation of a Pd(0) intermediate, alternative to **F**. At this point, BQ may exploit its oxidative power to restore a Pd(II) complex, an aspect, which has not been taken into account in the previous reports of this chemistry.[5]
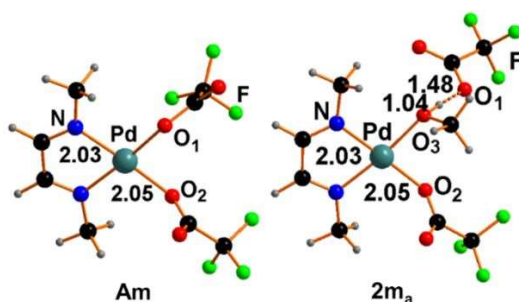
In this paper, we present an *in silico* investigation to highlight some still unclear aspects of the catalytic cycle of Scheme 2, which was constructed on the basis of the available experimental data. In particular, the approach helps shading some light on problematic features such as the role of the olefin R substituent (step **C→D**), the nature of the Pd species accompanying the release of the diester **P** and the function of the BQ oxidant in the process.

Results

As in previous studies of comprehensive catalytic cycles performed by us,[15] the DFT method was employed with the adoption of the B3LYP functional in this case.[16] The reliability of the various steps in Scheme 2 was questioned by series of full optimizations of minima and transition states. The results allowed the development of meaningful stereochemical and energetic arguments derived from the application to the frontier MOs of the qualitative perturbation theory.[17] The well experimentally characterized species were considered as the milestones of the overall catalytic pathway from which new indications were derived for the reconstruction of the entire process. Some modelling simplification helped to reduce the computational burden without introducing any major chemical bias. Thus, for the α-diimine N-N ligand **1a** (top of Scheme 2) methyl groups were used in place of the bulky dimethyl-phenyl ones and also the methyl substituent at the C atoms of the N=C-C=N skeleton were replaced by H atoms.[18] As another point, the bulk solvent (*i.e.,* a 7:1 mixture of methanol/THF in the experiments) was mimicked in the calculations as pure methanol within the approximation of the Conductor-like Polarized Continuum Model

4

(CPCM).[19] Otherwise, some actual CH_3OH molecule was explicitly introduced, when it is directly involved in the reactivity either as an intact or deprotonated ligand (*e.g.,* the transformation of Pd-O(H)CH_3 into Pd-OCH$_3$).
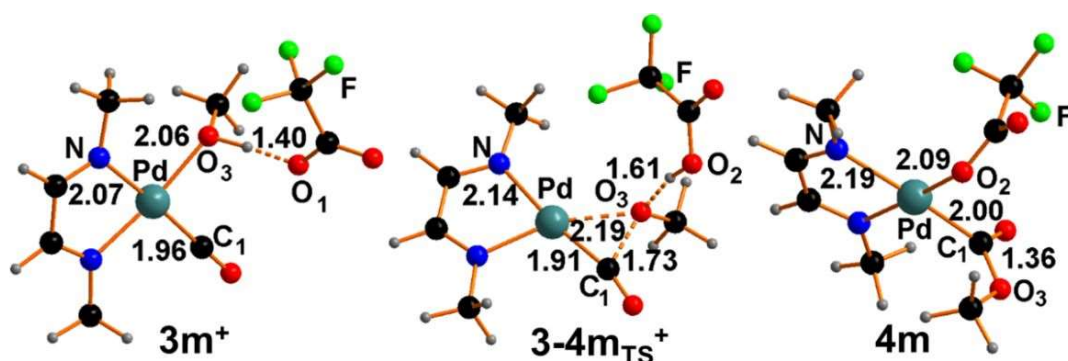
Formation of the Pd-alkoxycarbonyl intermediate (N-N)Pd(TFA)(C(O)OCH$_3$). The complex (N-N)Pd(TFA)$_2$, **A** in Scheme 2, was optimized as the simplified **Am** model at the left side of Figure 1. The geometry is substantially consistent with some known X-ray structure of this type[20] including that of the actual complex **A**.[5b] The potential steric effects in the latter should cause longer Pd-O distances with respect to **Am**, whereas in actuality the corresponding values are about 0.03 Å larger. Such an overestimation, also extended to the Pd-N coordination bonds, is therefore attributable to *pseudo*-potential adopted for the Pd atom in the DFT calculations.[21] The complex **Am** may evolve through the stepwise substitution of its TFA$^-$ ligands with other donors in solution such as for instance carbon monoxide, alkene (in the di–hapto bonding mode) or a methanol solvent molecule. As suggested in the literature,[7-9] methanol likely precedes the CO coordination to give the adduct [(N-N)Pd(TFA)(CH_3OH)]$^+$[TFA]$^-$, **2m$_a$** in Figure 1, where the two counterions are held together by a H-bonding interaction with O_3-H and H$^{..}O_1$ distances of 1.04 and 1.48 Å, respectively.

Figure 1. Optimized structures of the starting complex **Am** and the ion pair **2m$_a$**

The formation of the adduct **2m$_a$** is endergonic by +5.1 kcal mol^{-1}, since the entropy term overcomes the -5.6 kcal mol^{-1} favourable enthalpy one. The energy cost doubles for the formation of the adduct [(N-N)Pd(CH_3OH)$_2$]$^{+2}$·2[TFA]$^-$, **2m$_a$'** in Figure S1. However, the continuation of

5

the catalytic reactivity requires that the second TFA$^-$ ligand in **Am** is substituted by a CO

molecule to form the **3m**$^+$ cation (left side of Figure 2) with an energy cost of +9.5 kcal mol^{-1}. It

has been previously suggested,[22] that the order of the two TFA$^-$ substitutions with methanol and

CO could be reverse. In any case, the estimated +14.6 kcal mol^{-1} overall cost is independent from

the order of access of the two ligands. Most likely the CH$_3$OH coordination occurs first in view
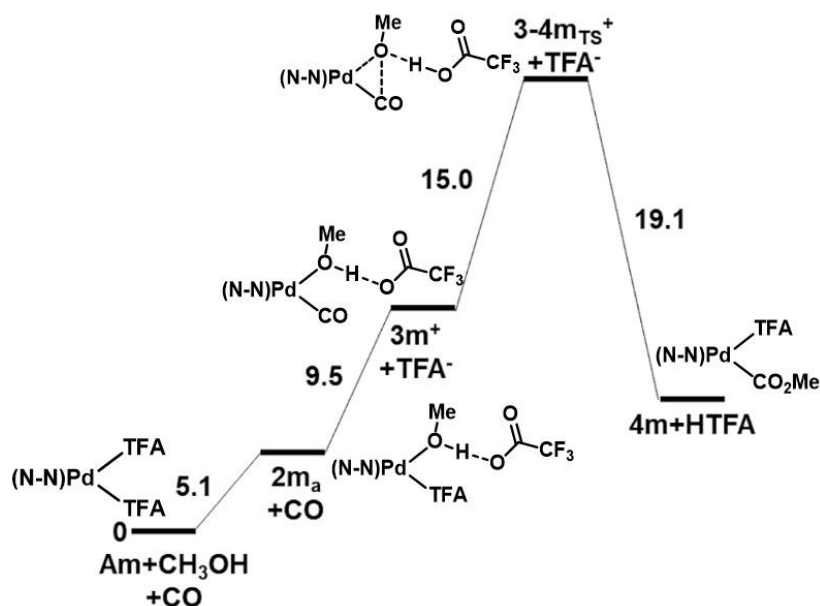
of the minor energy to be initially spent.

Figure 2. Cation **3m**$^+$ characterized by the CH$_3$OH ligand H-bonded to TFA$^-$; the transition state **3-4m**$_{TS}$$^+$ for the methoxo/CO coupling, which, thanks to the H transfer, implies a momentarily formed HTFA unit; intermediate **4m** with methoxycarbonyl and a TFA$^-$ ligands.

Next, the *cis* coordinated CO and CH$_3$OH molecules potentially couple together, provided a

proton transfer from the methanol O-H group to the carboxylate one of the adjacent TFA$^-$ anion.

The given H-bond persists only initially, but the H transfer has already occurred at the transition

state **3-4m**$_{TS}$$^+$ (in the centre of Figure 2), implying the inversion of the H-donor/acceptor

characters of methanol and TFA$^-$, respectively. The HTFA unit remains temporarily unsplit in

the polar methanol solvent, in spite of its strong acidic character. Incidentally, the latter and other

similar *in situ* formed units will play a basic role in the final part of the catalytic cycle. In turn,

the electron rich methoxo group has already started its transfer into carbon monoxide. In fact, the

C$_1$···O$_3$ distance is as short as 1.73 Å, while the Pd-O$_3$ linkage is weakened (2.19 Å). The process

is completed at the subsequent minimum **4m** (right side of Figure 3), where the C$_1$-O$_3$ bond is as

short as 1.36 Å. Such a product, described as the Pd-alkoxycarbonyl complex (N-

6

N)Pd(TFA)(C(O)OCH$_3$), has an *in situ* formed methoxycarbonyl ligand and a newly entered trifluoroacetate molecule.

As shown by the energy profile in Figure 3, the overall energy barrier at **3-4m$_{TS}^+$** is as high as +29.6 kcal mol^{-1}, because, relatively to **Am**, it includes the formation energies of both **2m$_a$** and **3m$^+$** plus the +15.0 kcal mol^{-1} necessary for the migration of the methoxo group to the CO ligand.

Figure 3. Free energy profile for the computed first part of the catalytic cycle corresponding to that in Scheme 2 (**A→C** or **Am → 4m**).

The height of overall barrier appears consistent with the observed slowness of the entire reaction (67 h), thus implying a rather long activation time of the catalyst. In the step from **3-4m$_{TS}^+$**, to **4m**, the system approximately recovers only two thirds of the initially spent energy (*i.e.,* -19.1 kcal mol^{-1}), implying that the efficiency of the process must be ensured by subsequent exergonic steps.

Activation and role of the mono-substituted olefins in the catalytic cycle. As already hypothesized for the step **C→D** in Scheme 2,[5] the TFA$^-$ ligand in **4m** can be potentially replaced by an olefin molecule of the type R^1-CH=CH-R^2 with R^1 = H or alkyl, R^2 = aryl, alkyl or EWG. In particular, in this paper we have focalized our attention on the bis-alkoxycarbonylation
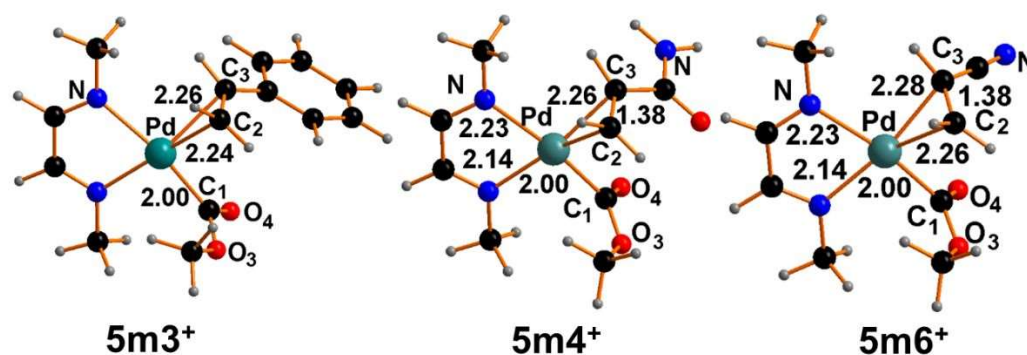
7

reaction of mono-substituted olefins (R^1 = H). In an attempt of justifying the experimental productivity observed for different olefins (see Table 2 of reference 5c and Table 2 of reference 5b), six Pd(II) complexes of general formula $(N-N)Pd(CO_2CH_3)(\eta^2-H_2C=CHR)$ were compared. In the optimized models **5m1$^+$-5m6$^+$**, the R substituent is H (ethylene **1**), CH_3 (propene **2**), Ph (styrene **3**), $CONH_2$ (acrylamide **4**), $COOCH_3$ (methyl acrylate **5**) and CN (acrylonitrile **6**), respectively. The formation of the species **5m1$^+$-5m6$^+$** from **4m** is invariably endergonic with the corresponding energy cost of +4.1, +5.0, +8.0, +8.3, +11.3 and +14.5 kcal mol^{-1}, respectively. These results suggest that in the series **5m3$^+$-5m6$^+$** the corresponding EWG substituents progressively disfavour the dihapto coordination of the olefin at variance with **5m1$^+$** and **5m2$^+$**, in which the R=H or CH_3 substituents determine a somewhat larger C=C donor power.[23] In fact, an increasing delocalization of the C=C π bonding electrons toward the EWG substituent implies a reduced σ donor power of the olefin toward the metal. In addition, the metal π back-donation from a T-shaped fragment of the d^8-L_3Pd(II) type, such as $[(N-N)Pd(COOCH_3)]^+$, is predictably scarce due to the small p_π-d_π orbital hybridization. This point is also corroborated by the almost null pinning back of the olefin terminal groupings at variance with the analogous complexes supported by a V-shaped d^{10}-L_2Pd(0) fragment.[24] As a matter of fact, not only the formation of all the species **5m1$^+$-5m6$^+$** result to be endergonic, but also the actually characterized L_3Pd(II)(η^2-olefin) structures are rare. For instance, the CCDC database[25] contains only one peculiar compound of this type, which may add the Pd(II) analogue of the Zeise's salt anion $[Cl_3Pd(\eta^2-H_2C=CH_2)]^-$.[26]

Although we try to compare up to six different olefins, experimental data are not available for ethylene and propene due to some technical reasons, which prevented their practical usage. Regarding the series **5m3$^+$-5m6$^+$**, the observed productivity increases in the order: acrylonitrile < methyl acrylate < acrylamide < styrene. In particular, styrene affords the highest yield associated to the lowest catalytic load. Indeed, with 0.5 mol% of catalyst loading, a complete

8

conversion of the styrene was achieved[5a] while acrylamide or methyl acrylate afforded a complete conversion of the olefin only for a catalyst load of 2 mol% and 3 mol%, respectively.[5c] It is worth underlining at this point that acrylonitrile is not only the least reactive olefin but it is essentially inactive,[5c] due to a poisoning effect (*vide infra*).
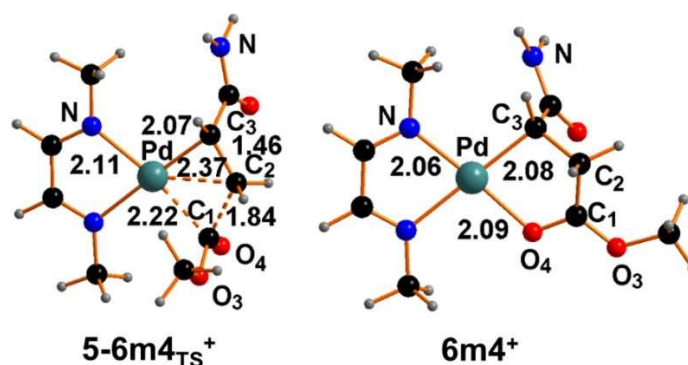
The structures of all the optimized models $5m1^+$-$5m6^+$ are geometrically rather similar, as shown in Figure 4 by the 3D drawings of $5m3^+$, $5m4^+$ and $5m6^+$ and all the others in Figure S2.

Figure 4. Optimized structures of the three comparative η^2-alkene complexes $5m3^+$ (styrene), $5m4^+$ (acryl amide) and $5m6^+$ (acrylonitrile).
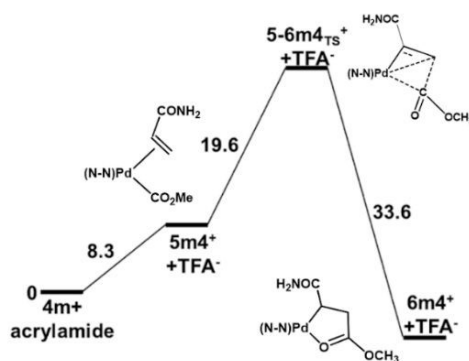
The complexes $5m3^+$ and $5m6^+$ display the highest difference in formation energy (+6.5 kcal mol^{-1}) consistently with their observed catalytic efficiency. Such a feature is not attributable to any evident structural divergence since the optimized Pd-C$_2$ and Pd-C$_3$ distances are inversely asymmetric by only 0.01-0.02 Å. To clarify the general evolution of the system, we monitored *via* scan techniques the progressive coupling of methoxycarbonyl C$_1$ atom and the C$_2$ one of the CH$_2$ grouping. In this manner, we individuated the possible transition state starting from the corresponding $5mn^+$ complexes with the only exclusion of $5m2^+$. Figure 5 shows the $5\text{-}6m4_{TS}^+$ transition state together with the subsequent minimum $6m4^+$, which features the *in situ* formed 5-membered palladacycle The other four pairs of analogues, which are presented in Figure S3, are geometrically quite comparable, since at the TS points the C$_1$···C$_2$ distance is in the range 1.84-1.87 Å, while both the Pd-C$_1$ and Pd-C$_2$ bonds are weakened, being in the ranges 2.20-2.22

9

and 2.34-2.38 Å, respectively. At the same time, the O_4 atom of the carboxo group progressively

becomes as the new donor to the metal given that the Pd$\cdots O_4$ distance shortens from 2.86 Å in **5-**
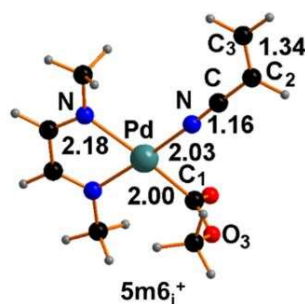
6m4$_{TS}^+$ to 2.09 Å in **6m4$^+$**.

Figure 5. Optimized structures of the transition state **5-6m4$_{TS}^+$** and the subsequent minimum **6m4$^+$**.

Five-membered palladacycles complexes similar to the determined **6mn$^+$** ones have been widely

described in the literature[10,11c-d,27] as key intermediates of the CO/alkene copolymerization

reactions.[28] On the other hand, our study shows that no major electronic effect is attributable to

the R substituent of the olefin. In fact, all of the five computed energy profiles feature a rather

similar TS barrier, which combines the formation energy of the olefin complex **5mn$^+$** and that of

the subsequent C-C coupling. In any case, the total energy barrier is in the relatively small range

+27.9/29.4 kcal mol^{-1}, the lowest value being common to both the acrylamide (**5m4$^+$**) and the

methyl acrylate (**5m5$^+$**) complexes. In view of the strict similarities, the energy profile in Figure

6 refers exclusively to the formation of the palladacycle **6m4$^+$** upon the reaction between the

complex **4m** and acrylamide**.**

Figure 6. Estimated free energy profile for the reaction of **4m⁺** with acrylamide to give the palladacycle **6m4⁺**.

The energy gains at the **6m1⁺** and **6m3⁺-6m6⁺** minima are instead more spread than those at the preceding TS points (namely, -28.9/-36.7 kcal mol⁻¹) with the largest value referring to the acrylonitrile derivative. However, the formation of the latter is excluded from the experimentally proven poisoning of the reactivity, as indicated in the literature.[5c,22a,29] Such a result is also confirmed by the optimized coordination isomer **5m6ᵢ⁺** of Figure 7, which by using the CN substituent forms a Pd-N σ linkage alternative to the C=C π one.

Figure 7. Optimized coordination isomer **5m6ᵢ⁺** with the acrylonitrile ligand bound *via* the terminal N atom.

The isomer in question is more stable than **5m6⁺** by -14.7 kcal mol⁻¹, thus greatly reducing the reformation of the η²-olefin complex, which could in principle occur via a shift of the equilibrium in solution. The latter argument receives some support from the acrylamide complex **5m4⁺**, given that its alternative isomer (**5m4ᵢ⁺** in Figure S4) with a Pd-O σ linkage formed by the CO group of the R substituent, is also more stable. In this case, the energy difference of only -2.3 kcal mol⁻¹
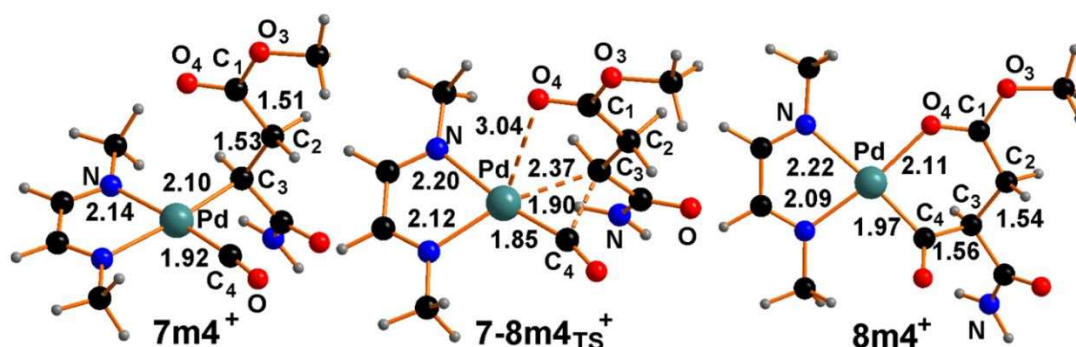
increases the possibility of an easier shift of the equilibrium in solution allowing a partial lifetime of the C=C dihapto coordination sufficient for the continuation of the catalysis. Also, the methyl acrylate derivative $5m5^+$ may have a similar behaviour, but the point was no further explored. On the other hand, since the best performing styrene derivative $5m3^+$ has no implicit problem of isomerization, it may be concluded that the R substituent of the olefin has no major electronic role in the catalysis. In conclusion, the reactivity is reduced depending on the σ bonding capability of R substituent, which may hinder the C=C π coordination at a different degree.

In closing this section, we briefly mention of having examined whether the bis-alkoxycarbonylation reactivity from a $5mn^+$ species involves either the CHR or CH_2 side of the olefin. In the former case, a 180° rotation of the dihapto bonded olefin is necessary. The structural rearrangement should be electronically feasible in view of the T-shaped nature of the underlying metal fragment carrying a pair of equivalent and pure d_π orthogonal orbitals. By referring to the $5m4^+$ species, the $5m4'^+$ conformer in question (shown in Figure S5) is destabilized by only +2.5 kcal mol^{-1}, due to the incipient steric contacts between the R group and the now closer alkoxycarbonyl ligand. The energy destabilization increases with the forcing of the $C_1 \cdots C_3$ coupling, as indicated by the corresponding barrier at $5\text{-}6m4_{TS}'^+$ (see Figure S6), which is about 30% higher than the one at $5\text{-}6m4_{TS}^+$ (+26.2 $vs.$ +19.6 kcal mol^{-1}). The result allows concluding that the olefin preferentially couples via its CH_2 grouping in agreement with some literature data, which show a generally preferred 2,1-olefin insertion in Pd-COR complexes.[10c,27a] Unfortunately, such a conclusion cannot be experimentally corroborated by the present chemistry due to the symmetric nature of the diester product **P**.

In summary, the variously substituted dihapto bonded olefins, which potentially lead to an intermediate of type **D** in Scheme 2 (*e.g.,* model $6m4^+$), feature substantially similar electronic and energetic behaviours. Conversely, the present study has shown how the experimentally observed difference in reactivity is due to the 2e$^-$ σ donor capability in the R group. By affording

12

a new coordination isomer either alternative or in equilibrium with the η^2-olefin complex, the catalytic cycle is either poisoned or inhibited.

Attainment of the immediate precursor of P. By momentarily disregarding the poisoning effect, all the di-hapto bonded R substituted olefins have a rather similar electronic behaviour. Accordingly, the acrylamide **6m4⁺** (right side of Figure 5) was used as the **D** type model of choice for the continuation of the catalytic cycle. In the latter, the previously formed *in situ* five-membered metallacycle opens the Pd-O_4 linkage, thus allowing the coordination of a new CO ligand as in the complex **7m4⁺** at the left side of Figure 8. Consequently, only the Pd-C_3 linkage survives with the alkoxycarbonyl group dangling away from the metal. Such a step has the small energy cost of only +2.1 kcal mol⁻¹.

Figure 8. Optimized structures of **7m4⁺**, the transition state for the alkyl-CO coupling **7-8m4$_{TS}$⁺** and the subsequent intermediate **8m4⁺**.

Then, **7m4⁺** undergoes a classical migration of the alkyl ligand to the adjacent CO one.[30] Again, a relaxed scan technique, based on the $C_3 \cdots C_4$ shortening, allowed both the identification and full optimization of the transition state **7-8m4$_{TS}$⁺** *plus* that of the subsequent minimum **8m4⁺** (see Figure 8). In the latter structure, the Pd-O_4 linkage, already present in **6m4⁺**, is restored with a slight elongation (*i.e.,* 2.11 *vs.* 2.09 Å), while an almost standard C_3-C_4 single bond of 1.56 Å is formed, after having been 1.90 Å long at the TS **7-8m4$_{TS}$⁺**. The corresponding energy barrier is +16.7 kcal mol⁻¹ with a subsequent recovery of -23.4 kcal mol⁻¹ at **8m4⁺**. The latter six-membered

13

metallacycle is also an intermediate of Pd-catalyzed copolymerization processes involving CO and alkenes.[7a, 27c] Such a species differs from the intermediate **E** of Scheme 2, which features a dangling acyl grouping and the fourth coordination site occupied by one TFA$^-$ anion. Incidentally, the corresponding optimized model **Em** (see Figure S7) has a +7.7 kcal mol^{-1} higher free energy with respect to the ion pair **8m4$^+$**/TFA$^-$ anion, as implied by an entropic effect. Nor, the TFA$^-$ coordination is essential for the continuation of the reactivity, since its prompt departure is necessary for the engagement of a methanol molecule needed to form the bis-alkoxycarbonylate product **P**, as described in the next section. Some computational work, concerning the coordination of a second CO molecule and its engagement in the bis-alkoxycarbonylation process, have been previously reported for the electron-deficient olefins.[5c]

Palladium behaviour in the formation of the di-ester product P. Similarly to the intermediates **2m$_a$** or **3m$^+$** in Figures 1 and 2, the H-bonding with TFA$^-$ anion better supports the metal coordination of a still intact CH$_3$OH molecule, which initially acts as a H donor. The proton is however transferred and forms a unit of the strong HTFA acid, thanks to a persisting H-bonding interaction with inverted roles of the H donor/acceptor groupings. As a matter of fact, the combined energy cost at **3-4m$_{TS}$$^+$** is the highest for the whole cycle (see Figure 3), then HTFA dissociates in the polar solution to form a methoxo ligand. A mechanism of the mentioned type also applies to the formation of the methoxo complex **9m4** (Figure 9) from **8m4$^+$** with an estimated energy cost of +12.5 kcal mol^{-1}.
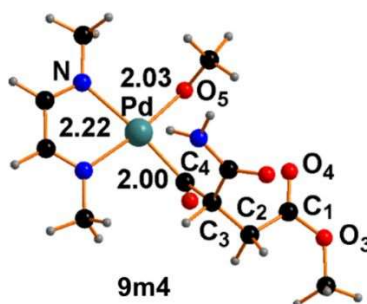
Figure 9. Optimized structure of **9m4** as the immediate precursor of the main product **P**.

By still referring to Scheme 2, the computed catalytic cycle encounters a main divergence in the

formation of the diester **P** for excluding the simultaneously formation of the hydride complex

(N-N)Pd(TFA)H, **F**. The latter species, also proposed by other authors[7c] to be an important

intermediate, has its own stability (see the optimized structure in Figure S8), but it is not

experimentally proved nor it justifies the formation of the covalent C_4-O_5 linkage. In fact,

provided the persisting +2 metal oxidation state, the corresponding lone pairs donated in **9m4**

promptly become repulsive to each other on cleaving the two coordination bonds. Hence, only if

one is captured by the metal (Pd(II)→Pd(0) reduction), the C_4-O_5 linkage may form. As an

additional consideration, the hydride ligand in **F** would result from a formal methanol heterolysis

with the CH_3O residue, that should couple with the acyl-type ligand to give **P**. All of the attempts

of confirming the latter hypothesis *via* scan techniques failed due to the high risings in energy (>

40 kcal mol^{-1}). In contrast, the Pd(II)→Pd(0) reduction, accompanied to the formation of **P** is

easily modelled as shown by Figure 10. Here, the progressive $C_4 \cdots O_5$ coupling leads first to the

TS **9-10m4$_{TS}$** with the small energy barrier of +6.2 kcal mol^{-1}, then the actual C_4-O_5 binding

allows **Pm** to separate from the (N-N)Pd(0) complex, **10m**. From the energy viewpoint, the

energy gain is small (-7.5 kcal mol^{-1}), because of the bent rather than linear geometry proper of

d^{10}-L_2M species. In this case, great stabilization is reached upon the addition of another ligand to

10m with formation of a highly stabilized trigonal planar geometry, as further discussed below.

It is worth underlining that the succinic product is not the result of a generally accepted

alcoholysis of the palladium-acyl bond (complex **E** in Scheme 2), but that of a reductive

elimination involving the methoxide and the acyl ligands of the precursor **9m4** (see Figure 9).
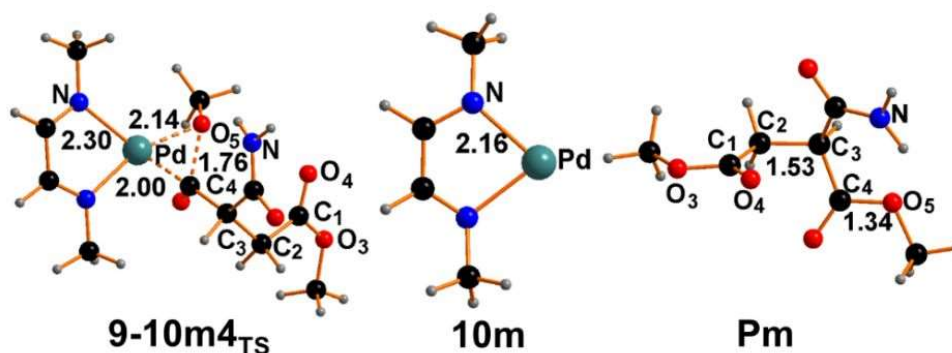
Figure 10. Optimized structures **9-10m4$_{TS}$**, **10m** and **Pm** proper of the reductive elimination process, which associates the formation of the succinate molecule with Pd(II)→Pd(0) reduction.

In closing this section, we present in Figure 11 the energy profile, whose features may be considered general, although the presented transformation from **4m** (Figure 2) to **Pm** and **10m** is estimated for acrylamide. Three progressively lower barriers are encountered, the highest one of +27.9 kcal mol^{-1} corresponding to the +8.3 and +19.6 kcal mol^{-1} sum. The values are relative to the olefin coordination (**5m4$^+$**) followed by the coupling of the H$_2$C moiety to the alkoxycarbonyl ligand (**6m4$^+$**), as shown in Figures 5 and 6. Then, a new CO coordination in **6m4$^+$** is smoother (+2.1 kcal mol^{-1}), while the subsequent alkyl migration into it encounters a +16.7 kcal mol^{-1} barrier at **7-8m4$_{TS}$$^+$**. The system recovers -23.4 kcal mol^{-1} on forming the six membered metallacycle at the minimum **8m4$^+$**, which seems suited for the activation and deprotonation of another methanol molecule in **9m4**. From the latter, the coupling between the methoxo and acyl ligands fundamentally implies the important reductive elimination step. As mentioned, an energy cost of only +6.2 kcal mol^{-1} is needed to bypass the TS **9-10m4$_{TS}$**, although the subsequent energy recovery for the simultaneous formation of **Pm** and **10m** is as small as -7.5 kcal mol^{-1}. At this point, the overall system is still endergonic by +11.4 kcal mol^{-1}, suggesting that, for the feasibility of the whole cycle, the steps for the restoration of the Pd(II) catalyst **Am** must be overwhelmingly exergonic. This is allowed by the efficiency of BQ as an oxidant.
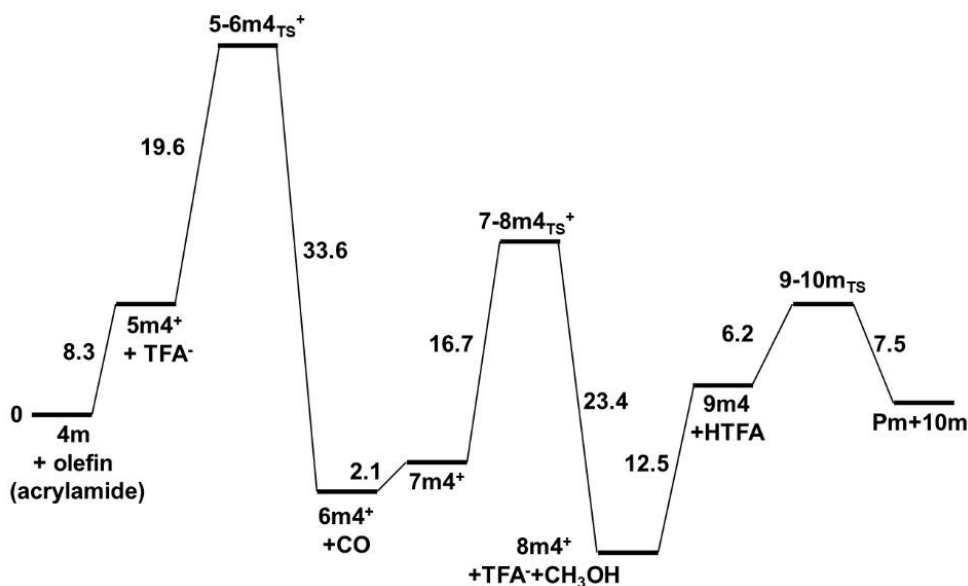
16

Figure 11. Summarized reaction profile for the portion of the cycle, which converts the alkoxycarbonyl/TFA complex **4m** into the (N-N)Pd(0) species **10m** together with di-ester product **Pm**.

Metal oxidation by the *p*-benzoquinone BQ to restore the catalyst (N-N)Pd(TFA)$_2$, Am.

A prompt stabilization of the (N-N)Pd(0) intermediate **10m** is possible with the addition of a third 2e$^-$ donor. For instance, CO forms the 16e$^-$ trigonal planar complex (N-N)Pd(CO) (Figure S9) with the large energy gain of -40.2 kcal mol^{-1}. More important for the continuation of the cycle is the di-hapto complex (N-N)Pd(η^2-BQ) (**11m** at left side of Figure 12), which exploits for bonding one C=C endocyclic linkage of BQ. In spite of the minor energy gain of -32.8 kcal mol^{-1}, BQ exerts its oxidative power and restores the actual Pd(II) catalyst **Am,** taken as the pre-catalyst of species **B** in Scheme 2.[5] The mechanism of the BQ action was already illustrated by one of us (*C.M.*) in a symbiotic experimental/theoretical investigation carried out with Giovanni Poli and co-workers.[14] In that case, the related catalyst (S-S)Pd(acetate)$_2$ (S-S = disulfoxide chelate PhS(=O)CH$_2$CH$_2$(O=)SPh)) was found to promote an intra-molecular C-N coupling, which allowed the reductive elimination of a cyclic allylic amine in association with the (S-S)Pd(0) unit and the subsequent BQ derivative (S-S)Pd(η^2-BQ). The latter species appear strictly comparable with the present **10m** and **11m** intermediates. In particular, a chemical

17

behaviour, analogous to that described by the computational analysis in reference 14, may be expected. More recently, the suggested mechanism has been validated also for another strictly related case.[31]
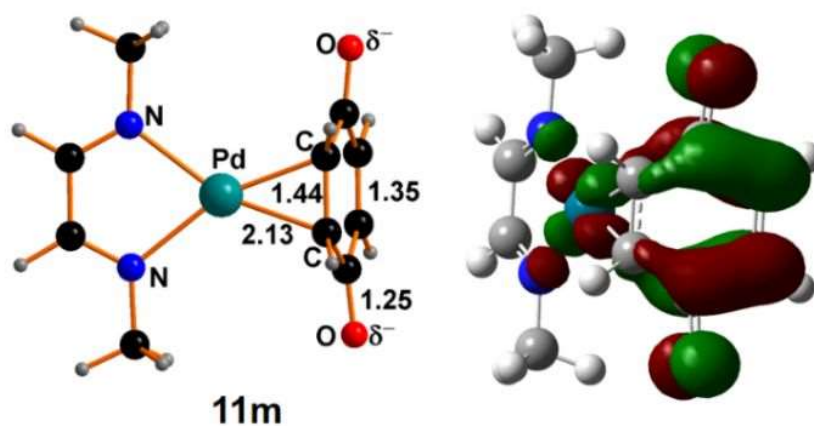
Figure 12. Trigonal planar complex (N-N)Pd(η^2-BQ), **11m**; the vacant frontier antibonding MO formed by one Pd-d_π orbital (populated) and a delocalized BQ-p_π combination.

Here, we report analogous DFT calculations to monitor the evolution of the Pd(0) complex **11m**, to check the presence of some peculiar specificity. In actuality, the catalyst regeneration is highly comparable in the two cases without necessarily implying the identity of all the single steps. It will emerge that some mechanistic specificity is introduced by the different strength (about 5 orders of magnitude) of the trifluoroacetic *vs*. the acetic acid used in the two cases.

Complex **11m**, of which there are analogues in the literature,[13,22] is characterized by the conformation and electron richness of the Pd(0) metal. This ensures a significant d_π back-donation delocalized over the BQ molecule, as corroborated by the vacant π antibonding frontier MO at the right side of Figure 12. The involvement of the BQ exocyclic oxygen atoms is confirmed by their -0.15 more negative charge with respect to the free molecule. Accordingly, bilateral H-linkages with HTFA units are possible, as shown by the schematized adduct (N-N)Pd(BQ)·2CF$_3$COOH, **12m** in Figure 13, which has gained -7.5 kcal mol^{-1} (its ball and stick structure is presented in Figure S10).
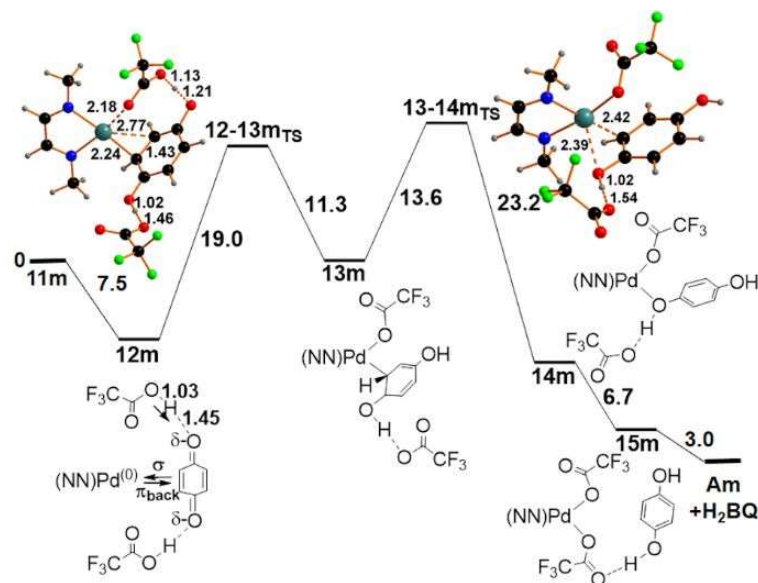
18

Figure 13. The Pd(0)$\rightarrow$Pd(II) oxidation path, which, by involving the sacrificial BQ molecule, leads to the separated hydroquinone H$_2$Q and the **Am** catalyst. All the schematized minima of the lower part of the figure are reported as ball and stick models in Figures S10-S13.

While in both **11m** and **12m** the metal is undoubtedly Pd(0), the oxidation state seems already changed at the TS **12-13m$_{TS}$**. For instance, one HTFA proton, already transferred to a BQ oxygen atom, affords the first O-H substituent at the C$_6$ ring (O-H = 1.02 Å) with maintained H-bonding interaction. In the latter, the H-donor/H-acceptor characters of the involved groupings have been switched, certainly implying an already reduced phenoxo anion. Also, a similar but less pronounced event is occurring at the other BQ oxygen atom, since the HTFA proton forms a O-H$^{..}$O grouping with the almost similar distances of 1.13 and 1.21 Å, respectively. Therefore, the TS **12-13m$_{TS}$**, which is destabilized by +19.0 kcal mol^{-1}, appears as a milestone of the redox process. The structure already features an advanced $\eta^2\rightarrow\eta^1$ conversion of the C=C binding mode as well as metal coordination of one TFA$^-$ anion (Pd-O = 2.18 Å). The indicated trends are completed at the next minimum **13m** (Figure S11), which features a doubly O-H substituted C$_6$ ring with the implicit aromaticity of the 1,4-hydroquinone (H$_2$BQ). At this point, the metal oxidation has definitely occurred, also because it is known that L$_3$Pd(II) fragments may attain approximate square planar geometry *via* the η^1-coordination of an aryl ring.[32] Such a type of

bonding was computationally explored in a previous paper, which indicated how a fraction of the six π electrons of an aromatic C_6 ring partially localizes at a single C atom to saturate the d^8 atom.[32a]

Provided that the metal oxidation has already occurred at **13m**, the system should release the η^1 bound H_2BQ molecule to be replaced by a second TFA[-] ligand as in the **Am** catalyst. The calculations indicate that such a process is not so straightforward, due to a relatively stabilizing η^1 coordination of H_2BQ. In fact, +13.6 kcal mol^{-1} must be spent to reach the TS **13-14m_TS**, in which the C_6 ring is still somewhat bound to the metal. At this point, the metal is approximately five-coordinated thanks to the two weak bonds, *i.e.,* to the unique C atom of the ring (Pd-C = 2.42 Å) and to the exocyclic OH group (Pd-O = 2.39 Å). At the next minimum **14m**, the aryl ligand is no more C-coordinated having been replaced by one H_2BQ phenolic moiety with a stabilization energy of -23.2 kcal mol^{-1}. Notice that the binding of the HOAr moiety in **14m** compares with the methanol one in **2m_a** or **3m[+]** of Figures 1 and 2. Finally, the second TFA[-] ligand directly coordinates the metal in **15m**, where the restored **Am** catalyst is still H-bound to H_2BQ with an energy gain of -6.7 kcal mol^{-1}. The final separation of the latter components determines an additional energy gain of -3.0 kcal mol^{-1}, as shown at the right side of Figure 13.

The overall energy balance for the portion of the cycle in Figure 13 is -19.1 kcal mol^{-1}, a value, which compares with the -12.2 kcal mol^{-1} estimated for the evolution of the (S-S)Pd(η^2-BQ) analogue.[14] In addition to the energy, some geometry difference is noticed for the intermediates and TS of the two systems, which is likely due to the usage of the CH_3COOH acid *vs.* the HTFA one. In particular, the much weaker acetic acid has a more propensity to remain unsplit, thus preferentially behaving as a H-donor rather than a H-acceptor in some H-bonding interactions, For instance, the structures **13-14m_TS** and **14m** of Figure 13 with a metal bound OH substituent differ from those observed in the presence of the acetic acid. The latter feature a direct bond between the unprotonated phenoxo O atom and the metal center.[14] Only the coordination of the

second acetate ligand (as in the case of the analogue **15m** in Figure 13) eventually favours the actual H_2BQ formation. Based on the previously illustrated arguments, it appears that the stronger HTFA acid performs better than the acetic one in the critical restoration of the catalyst.[33]

The electronic redistribution in the BQ metal re-oxidation has been already outlined,[14] hence only some additional consideration is presented here. The Pd(0)→Pd(II) transformation seems to occur at a very early stage, possibly even before the attainment of **12-13m$_{TS}$**. At the latter, the $\eta^2 \rightarrow \eta^1$ rearrangement of the C=C endocyclic π linkage is already advanced, consistently with the stability of known Pd(II) complexes featuring a η^1 coordinated aryl ring. Also, the exocyclic O atoms have already acquired a phenoxo character, since one of them is already protonated and the other one is also on this way. Scheme 3 illustrates the intended electron redistribution starting from the Pd(0) complex $L_2Pd(\eta^2-BQ)$, **11m** , indicated as the model **a**.[34] The latter picture involves a significant metal d_π back-donation, hence it is presumable that toward the C=C η^1 coordination the filled metal orbital undergoes a $d_\pi \rightarrow \sigma$ re-hybridization with a continuing electron flow into one vacant C_6 level (**b** model in Scheme 3). Such a situation would comply with the recently introduced concept of Inverted Ligand Field,[35] which assigns a M-C bonding electron pair to the metal rather than the ligand as a donor (σ back-donation). In this specific case, the inverted gap between the metal and ligand levels is quite transitory especially with respect to the behaviour of coinage metal.[35, 36] Consequently, a quick interchange of the donor and acceptor levels determines a prompt assignment of the bonding electrons to the carbon atom of the ring, as suggested by the model **c**. The exceeding electron pair at the BQ molecule are promptly redistributed at the terminal O atoms, allowing the C_6 ring to become fully aromatic as shown by model **d**. From the latter, the metal coordination of the second TFA$^-$ ligand restores the **Am** catalyst as already outlined for the last two steps of Figure 13. In summary, an indication of the energy cost for the Pd(0)→Pd(II) redox process likely identifies with the **12-13m$_{TS}$** barrier,

although an even earlier occurrence may be supported by the prompter change of the C_6 ring

coordination mode.
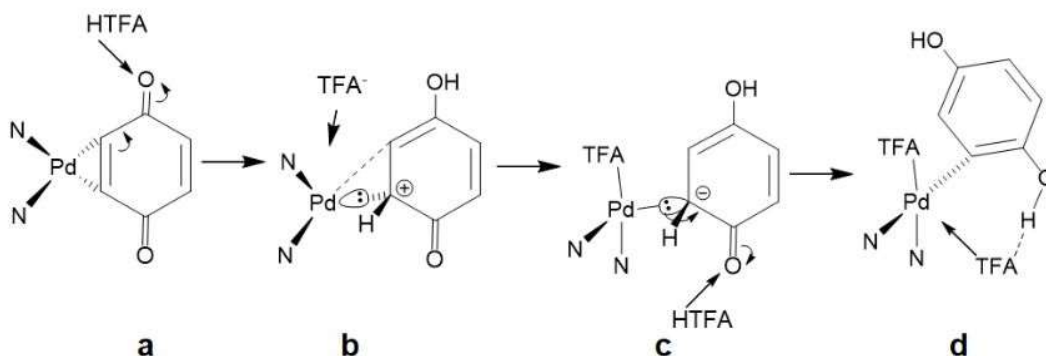
Scheme 3. Qualitative description of the electron redistribution in going the Pd(0) complex **11m** (**a**) to the Pd(II) adduct (N-N)Pd(II)TFA·H_2BQ **15m** (**d**).

The proposed oxidation of Pd(0) to Pd(II) in the transformation from (N-N)Pd(η^2-BQ) to

(N-N)Pd(TFA)$_2$ is also consistent with the results of previous NMR studies.[22]

Conclusions

The structural, electronic and energetic response of the DFT study corroborates several of the

intermediates proposed for the catalytic cycle of Scheme 2.[5] On the other hand, it has emerged

that the cycle shown in Scheme 4 provides a definitely more reliable overview of the process,

that implies an overall free energy balance of -22.7 kcal mol^{-1}. This value results from all the

basic steps, already described in details, which jointly afford the restoration of the actual catalyst

(N-N)Pd(TFA)$_2$, **Am**. The latter was instead indicated as a pre-catalyst in Scheme 2.
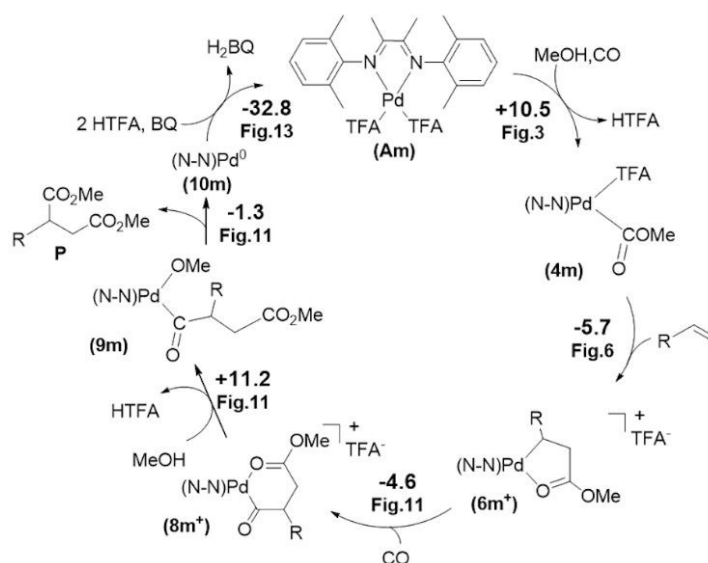
Scheme 4. Overall catalytic cycle for the bis-alkoxycarbonylation of mono-substituted olefins. The computed free energy balance in kcal·mol^{-1} is reported for any single step together with the Figure number presenting the corresponding detailed profile.

Numerous reactants are involved in the bis-alkoxycarbonylation process, such as olefin, carbon monoxide, methanol and *p*-benzoquinone. In particular, it emerges that the choice of the R substituent of the CH$_2$=CHR olefin plays a critical role. Indeed, from the available experimental data, a different R group considerably affects the productivity of the carbonylation process. With relation to this, no evidence of major electronic effects emerges by assuming that the olefin can attain a dihapto coordination mode to the metal. However, a 2e$^-$ donor of different power in the R substituent may affect the efficiency of the catalyst up to its complete poisoning. As an example, acrylonitrile may form a rather stable derivative with its CN group σ coordinated to the metal. This prevents the expected evolution of the process, which may start from the π coordinated C=C linkage in agreement with the experimental inhibition of the reactivity.[5c] In other cases, the R group with a weaker 2e$^-$ donor determines a small energy difference between the σ or π bound isomers. This helps balancing the equilibrium in solution, affording a sufficient lifetime of the dihapto complex for continuing the catalytic formation of **P** (*e.g.,* the acrylamide derivative[5c]).

At variance with previous proposals,[5,7c] the present *in silico* analysis shows that the formation of the diester **P** in no case accompanies to the generally accepted genesis of a Pd(II)-hydride complex. Not only the latter was safely excluded in view of its high energy costs but also because the persistent Pd(II) species would rule out the fundamental reductive elimination step. Only the latter affords the formation of the methoxo/acyl covalent bond in the succinate product. Conversely, the reduced (N-N)Pd(0) intermediate may continue the cycle by forming the d^{10} trigonal planar complex (N-N)Pd(η^2-BQ), **11m**, which directly involves the benzoquinone reactant. In fact, BQ may exert its oxidative action aimed to restore the original Pd(II) catalyst, **Am**. The paper has illustrated the $2e^-$ transfer from the reduced metal to BQ *via* a $\eta^2 \rightarrow \eta^1$ rearrangement of one endocyclic C=C linkage. In this manner, the original d_π metal back-donation transforms into a σ type one with the two bonding electrons being transitorily assigned to the metal (Inverted Ligand Field concept[35]). Then, the electron pair is promptly transferred to BQ, which is sacrificially reduced and protonated to give the hydroquinone product. In fact, similarly to what was previously found,[13,14] the process is assisted by H-bonding networks, which in this case involves the trifluoroacetic acid. The latter is generated *in situ* upon the methanol's deprotonation by the trifluoroacetate ligands, originally forming the catalyst **Am**. Since HTFA is definitely stronger than the acetic acid (previously found to accelerate a strictly related process[14]), it allows a greater efficiency of the catalysis.

The insights into the mechanism of the bis-alkoxycarbonylation process of a terminal olefin may be usefully extended to other carbonylation reactions or CO/olefin copolymerization, which similarly utilize alkene substrates together with the benzoquinone oxidant. As further developments of this chemistry, we plan to deepen our understanding of the steric/electronic factors, by focusing in particular on the role of the substituents at the α-diimine ligand as well as on the effect of various alcohols either as solvent or added reagent.[5b]

COMPUTATIONAL DETAILS

All of the models were optimized at the B3LYP-DFT level of theory[16] by using the Gaussian 09 package.[37] All the optimized structures were validated as minima and/or transition states by vibrational frequencies. All the calculations were based on the CPCM model[19] for mimicking the experimentally used methanol solvent. The effective Stuttgart/Dresden basis set (SDD)[21] was adopted for palladium, while the basis set 6-31G with the polarization functions (d, p) was employed for all the other atoms. Qualitative MO arguments have been developed with the help of the EHMO analysis performed with the CACAO package,[17] after ensuring that the wave functions are sufficiently consistent with the DFT ones. The coordinates as well as the energetic features of all the optimized structures are reported in the Supporting Information.

AUTHOR INFORMATION

Corresponding Author
*Email: gmanca@iccom.cnr.it (Gabriele Manca)

ORCID
Carlo Mealli: 0000-0002-7130-1076
Gabriele Manca: 0000-0003-2068-1731
Riccardo Tarroni: 0000-0001-6439-9979
Diego Olivieri: 0000-0001-9411-4487
Carla Carfagna: 0000-0002-3761-6920

NOTES
The authors declare no competing financial interest.

ASSOCIATED CONTENT

The Supporting Information contains the coordinates and energetic parameters of all the

optimized models in this study and the structures of some intermediates of the catalytic

cycle.

References

(1)   (a) Beller, M. *Catalytic Carbonylation Reactions*, Springer, Berlin, **2006**. (b) Kollär, L. *Modern Carbonylation Methods*, Wiley-VCH, Weinheim, **2008**. (c) Omae, I. Transition metal-catalyzed cyclocarbonylation in organic synthesis. *Coord. Chem. Rev.* **2011**, *255*, 139-160. (d) Wu, X.-F.; Neumann, H. Ruthenium and Rhodium-Catalyzed Carbonylation Reactions. *ChemCatChem* **2012**, *4*, 447-458. (e) Wu, L.; Fang, X.; Liu, Q.; Jackstell, R.; Beller, M.; Wu, X.-F. Palladium-Catalyzed Carbonylative Transformation of $C(sp^3)$–X Bonds. *ACS Catal.* **2014**, *4*, 2977-2989. (f) Gehrtz, P. H.; Hirschbeck, V.; Ciszek, B.; Fleischer, I. Carbonylations of Alkenes in the Total Synthesis of Natural Compounds. *Synthesis* **2016**, *48*, 1573-1596. (g) Friis, S. D.; Lindhardt, A. T.; Skrydstrup, T. The Development and Application of Two-Chamber Reactors and Carbon Monoxide Precursors for Safe Carbonylation Reactions. *Acc. Chem. Res.* **2016**, *49*, 594-605. (h) Wu, X.-F.; Beller, M. *Transition Metal Catalyzed Carbonylative Synthesis of Heterocycles in Topics in Heterocyclic Chemistry Vol. 42*, Springer, **2016**. (i) Shen, C.; Wu, X.-F. Palladium-Catalyzed Carbonylative Multicomponent Reactions. *Chem. – Eur. J.* **2017**, *23*, 2973-2987. (j) Peng, J.-B.; Geng, H.-Q.; Wu, X.-F. The Chemistry of CO: Carbonylation. *Chem.* **2019**, *5*, 526-552.

(2)   (a) Hethcox, J. C.; Shanahan, C. S.; Martin, S. F. Total synthesis of (−)-dihydroprotolichesterenic acid via diastereoselective conjugate addition to a chiral fumarate. *Tetrahedron Letters* **2013**, *54*, 2074-2076. (b) Sibi, M. P.; Hasegawa, H. An Efficient Method for Synthesis of Succinate-Based MMP Inhibitors. *Org. Lett.* **2002**, *4*, 3347-3349. (c) Whittaker, M.; Floyd, C. D.; Brown, P.; Gearing, A. J. H. Design and Therapeutic Application of Matrix Metalloproteinase Inhibitors. *Chem. Rev.* **1999**, *99*, 2735-

2776. (d) Kammermeier, B.; Beck, G.; Holla, W.; Jacobi, D.; Napierski, B.; Jendralla, H. Vanadium(II)- and Niobium(III)-Induced, Diastereoselective Pinacol Coupling of Peptide Aldehydes to Give a C_2-Symmetrical HIV Protease Inhibitor. *Chem. -Eur. J.* **1996**, *2*, 307-315. (e) Jendralla, H. Asymmetric hydrogenation of itaconic acids with rhodium(I)-phenyl-capp complex a correction. *Tetrahedron Lett.* **1991**, *32*, 3671-3672. (f) Ito, Y.; Kamijo, T.; Harada, H.; Matsuda, F.; Terashima, S. An efficient synthesis of methyl *N*-[2-(*R*)-(1-napthylmethyl)-3-(morpholinocarbonyl)propionyl]-(*S*)-histidinate, the key synthetic intermediate of renin inhibitors. *Tetrahedron Lett.* **1990**, *31*, 2731-2734. (g) Yoshikawa, K.; Inoguchi, K.; Morimoto, T.; Achiwa, K. Preparation of Newly Modified DIOP Bearing Bis(4-dimethylamino-3,5-dimethylphenyl)phosphino Groups and Its Application to Efficient Asymmetric Hydrogenation of Itaconic Acid Derivatives. *Heterocycles* **1990**, *31*, 1413-1416.

(3)   For examples concerning the use of succinates as plasticizers, see: (a) Jamarani, R.; C. Erythropel, H.; Burkat, D.; Nicell, J. A.; Leask, R. L.; Maric, M. Rheology of Green Plasticizer/Poly(vinyl chloride) Blends via Time–Temperature Superposition. *Processes* **2017**, *5*, 43-56. (b) Erythropel, H. C.; Dodd, P.; Leask, R.; Maric, M.; Cooper, D. G. Designing green plasticizers: Influence of alkyl chain length on biodegradation and plasticization properties of succinate based plasticizers. *Chemosphere* **2013**, *91*, 358-365. (c) Stuart, A.; LeCaptain, D. J.; Lee, C. Y.; Mohanty, D. K. *Eur. Polym. J.* **2013**, *49*, 2785- 2791. (d) Stuart, A.; McCallum, M. M.; Fan, D.; LeCaptain, D. J.; Lee, C. Y.; Mohanty, D. K. Poly(vinyl chloride) plasticized with succinate esters: synthesis and characterization. *Polym. Bull.* **2010**, *65*, 589-598. For uses of succinates as monomers in polymers or dendrimers, see: (e) Jiang, Y.; Woortman, A. J. J.; van Ekenstein, G. O. R. A.; Loos, K. Enzyme-Catalyzed Synthesis of Unsaturated Aliphatic Polyesters Based on Green Monomers from Renewable Resources. *Biomolecules* **2013**, *3*, 461-480. (f) Hevus, I.; Pikh, Z. Novel Surface-Active Succinate Monomers and Initiators for Obtaining Reactive Polymers**.** *Macromol. Symp.* **2007**, *254*, 103-108. (g) Carnahan, M. A.; Grinstaff, M. W. Synthesis of Generational Polyester Dendrimers Derived from Glycerol and Succinic or Adipic Acid. *Macromolecules* **2006**, *39*, 609-616. (h) Carnahan, M. A.; Grinstaff, M. W. Synthesis and Characterization of Poly(glycerol−succinic acid) Dendrimers**.** *Macromolecules* **2001**, *34*, 7648-7655.

(4)   For selected reviews concerning oxidative carbonylation reactions, see: (a) Wu, X.-F.; Neumann, H.; Beller, M. Palladium-Catalyzed Oxidative Carbonylation Reactions. *ChemSusChem* **2013**, *6*, 229-

241. (b) Gabriele, B.; Mancuso, R.; Salerno, G. Oxidative Carbonylation as a Powerful Tool for the Direct Synthesis of Carbonylated Heterocycles. *Eur. J. Org. Chem.* **2012**, 6825-6839. (c) Liu, Q.; Zhang, H.; Lei, A. Oxidative Carbonylation Reactions: Organometallic Compounds (R-M) or Hydrocarbons (R-H) as Nucleophiles. *Angew. Chem.* **2011**, *123*, 10978-10989; *Angew. Chem. Int. Ed.* **2011**, *50*, 10788-10799. (d) Gabriele, B.; Salerno, G.; Costa, M. Oxidative Carbonylations. *Top. Organomet. Chem.* **2006**, *18*, 239-272.

(5)   (a) Fini, F.; Beltrani, M.; Mancuso, R.; Gabriele, B.; Carfagna, C. Selective Aryl alpha-Diimine/Palladium-Catalyzed Bis-Alkoxy- carbonylation of Olefins for the Synthesis of Substituted Succinic Diesters. *Adv. Synth. Catal.* **2015**, *357*, 177-184. (b) Olivieri, D.; Fini, F.; Mazzoni, R.; Zacchini, S.; Della Ca', N.; Spadoni, G.; Gabriele, B.; Mancuso, R.; Zanotti, V.; Carfagna, C. Diastereospecific Bis-alkoxycarbonylation of 1,2-Disubstituted Olefins Catalyzed by Aryl α-Diimine Palladium(II) Catalysts. *Adv. Synth. Catal.* **2018**, *360*, 3507-3517. (c) Olivieri, D.; Tarroni, R.; Della Ca', N.; Mancuso, R.; Bartolo, G.; Spadoni, G.; Carfagna, C. Bis-Alkoxycarbonylation of Acrylic Esters and Amides for the Synthesis of 2-Alkoxycarbonyl or 2-Carbamoyl Succinates. *Adv. Synth. Catal.* **2020**, *362*, 533-544.

(6)   Using terminal olefins as substrate slightly higher yields were obtained with the ligand N^2,N^3-di(anthracen-9-yl)butane-2,3-diimine, while the ligand N^2,N^3-bis(2,6-dimethylphenyl)butane-2,3-diimine (**1a**) gave better results with 1,2-disubstituted alkenes or electron-deficient olefins.

(7)   (a) Drent, E.; Budzelaar, H. M. Palladium-Catalyzed Alternating Copolymerization of Alkenes and Carbon Monoxide. *Chem. Rev.* **1996**, *96*, 663-681. (b) Vavasori, A.; Toniolo, L. Carbon monoxide-ethylene copolymerization catalyzed by a Pd(AcO)$_2$/dppp/TsOH system: the promoting effect of water and of the acid. *J. Mol. Catal. A* **1996**, *110*, 13-23. (c) Bianchini, C.; Lee, H. M.; Mantovani, G.; Meli, A.; Oberhauser, W. Bis-alkoxycarbonylation of styrene by pyridinimine palladium catalysts. *New J. Chem.* **2002**, *26*, 387-397.

(8)   Intermediates analogous to **B** have been previously identified in olefin carbonylation processes conducted in the presence of BQ and MeOH as solvent. For examples see: (a) Sperrle, M.; Consiglio, G. Olefin Carbonylation Catalysis with Cationic Palladium Complexes: Selectivity and Possible Intermediates. *Chem. Ber.* **1997**, *130*, 1557-1565. (b) Bianchini, C.; Mantovani, G.; Meli, A.; Oberhauser, W.; Brüggeller, P.; Stampfl, T. Novel diphosphine-modified palladium catalysts for oxidative

carbonylation of styrene to methyl cinnamate. *J. Chem. Soc., Dalton Trans.* **2001**, 690-698. (c) Liu, J.; Heaton, B. T.; Iggo, J. A.; Whyman, R. The Complete Delineation of the Initiation, Propagation, and Termination Steps of the Carbomethoxy Cycle for the Carboalkoxylation of Ethene by Pd–Diphosphane Catalysts. *Angew. Chem. Int. Ed.* **2004**, *43*, 90-94.

(9)   For CO insertion reactions into the Pd-OMe bond, see: (a) Smith, G. D.; Hanson, B. E.; Merola, J. S.; Waller, F. J. Palladium methoxide and carbomethoxy complexes: synthesis and molecular structure of (bipy)Pd(CO$_2$CH$_3$)$_2$. *Organometallics* **1993**, *12*, 568-570. (b) Kapteijn, G. M.; Verhoef, M. J.; van den Broek, M. A. F. H.; Grove, D. M.; van Koten, G. Carbonylation of diamino-ligated methylpalladium(II) methoxide complexes. *J. Organomet. Chem.* **1995**, *503*, C26-C28. (c) Kapteijn, G. M.; Dervisi, A.; Verhoef, M. J.; van den Broek, M. A. F. H.; Grove, D. M.; van Koten, G. Chemistry of diamino-ligated methylpalladium(II) alkoxides and aryloxides (Part II): methoxide formation and carbonylation reactions. *J. Organomet. Chem.* **1996**, *517*, 123-131.

(10)   (a) Binotti, B.; Carfagna, C.; Gatti, G.; Martini, D.; Mosca, L.; Pettinari, C. Mechanistic Aspects of Isotactic CO/Styrene Copolymerization Catalyzed by Oxazoline Palladium(II) Complexes. *Organometallics* **2003**, *22*, 1115-1123. (b) Carfagna, C.; Gatti, G.; Mosca, L.; Paoli, P.; Guerri, A. Synthesis of a Novel a -Diimine Palladium(II) Complex Bearing an η^3-Allyl γ -Lactone Ligand, a Key Intermediate in Alkyne Cyclocarbonylation Processes. *Organometallics* **2003**, *22*, 3967-3970. (c) Carfagna, C.; Gatti, G.; Mosca, L.; Natanti, P.; Paoli, P.; Rossi, P.; Gabriele, B.; Salerno, G. Carbonylation of styrenes catalyzed by bioxazoline Pd(II) complexes: mechanism of enantioselectivity. *Dalton Trans.* **2011**, *40*, 6792-6801.

(11)   When an olefin bearing an aryl group is employed, the formation of an η^3-allylic Pd-intermediate cannot be ruled out. For examples, see: (a) Carfagna, C.; Gatti, G.; Paoli, P.; Binotti, B.; Fini, F.; Passeri, A.; Rossi, P.; Gabriele, B. New Aryl α-Diimine Palladium(II) Catalysts in Stereocontrolled CO/Vinyl Arene Copolymerization. *Organometallics* **2014**, *33*, 129-144. (b) Rix, F. C.; Rachita, M. J.; Wagner, M. I.; Brookhart, M.; Milani, B.; Barborak, J. C. Palladium(II)-catalyzed copolymerization of styrenes with carbon monoxide: mechanism of chain propagation and chain transfer. *Dalton Trans.* **2009**, *42*, 8977-8992. (c) Carfagna, C.; Gatti, G.; Paoli, P.; Rossi, P. Mechanism for Stereoblock Isotactic CO/Styrene Copolymerization Promoted by Aryl α-Diimine Pd(II) Catalysts: A DFT Study. *Organometallics* **2009**,

28, 3212-3217. (d) Carfagna, C.; Gatti, G.; Mosca, L.; Passeri, A.; Paoli, P.; Guerri, A. Stereocontrol mechanism in CO/*p*-methylstyrene copolymerisation catalysed by aryl-α-diimine Pd(II) complexes**.** *Chem. Commun.* **2007**, *43*, 4540-4542.

(12)　　It has been proposed that in the presence of CH₃OH and an oxidant, Pd-H species are generally oxidized to Pd-OMe complexes; for examples see: Eastham, G. R.; Heaton, B. T.; Iggo, J. A.; Tooze, R. P.; Whyman, R.; Zacchini, S. Synthesis and spectroscopic characterisation of *all* the intermediates in the Pd-catalysed methoxycarbonylation of ethene. *Chem. Commun.* **2000**, 609-610 and reference 7.

(13)　　For the role of BQ in the regeneration of a Pd(II) complex from a Pd(0) species, see: Grennberg, H.; Gogoll, A.; Baeckvall, J.-E. Acid-induced transformation of palladium(0)-benzoquinone complexes to palladium(II) and hydroquinone**.** *Organometallics* **1993**, *12*, 1790-1793.

(14)　　(a) Nahra, F.; Liron, F.; Prestat, G.; Mealli, C.; Messaoudi, A.; Poli, G. Striking AcOH Acceleration in Direct Intramolecular Allylic Amination Reactions. *Chem.-Eur. J.* **2009**, *15*, 11078-11082. (b) Lorion, M. M.; Nahra, F., LY, V. L.; Mealli, C.; Messaoudi, A.; Liron, F-; Oble, J.; Poli, G. Digging into the mechanism of oxidative Pd(II)-catalyzed aminations. *Chimica Oggi-Chemistry Today* **2014**, *32*, 30-34.

(15)　　(a) Carrasco, C. J.; Montilla, F.; Alvarez, E.; Mealli, C.; Manca, G.; Galindo, A. Experimental and theoretical insights into the oxodiperoxomolybdenum-catalysed sulphide oxidation using hydrogen peroxide in ionic liquids. *Dalton Trans***.** **2014**, *43*, 13711-13730. (b) Zardi, P.; Pozzoli, A.; Ferretti, F.; Manca, G.; Mealli, C.; Gallo, E. A mechanistic investigation of the ruthenium porphyrin catalysed aziridination of olefins by aryl azides. *Dalton Trans***.** **2015**, *44*, 10479-10489. (c) Manca, G.; Gallo, E.; Intrieri, D.; Mealli, C. DFT Mechanistic Proposal of the Ruthenium Porphyrin-Catalyzed Allylic Amination by Organic Azides. *ACS Catal.* **2014**, *4*, 823-832. (d) Intrieri, D.; Carminati, D. M.; Zardi, P.; Damiano, C.; Manca, G.; Gallo, E.; Mealli, C. Indoles from Alkynes and Aryl Azides: Scope and Theoretical Assessment of Ruthenium Porphyrin-Catalyzed Reactions. *Chem.-Eur. J.* **2019**, *25*, 16591-16605.

(16)　　(a) Becke, A. D. Density-functional thermochemistry. III. The role of exact exchange. *J. Chem. Phys.* **1993**, *98*, 5648-5652. (b) Lee, C.; Yang, W.; Parr, R. G. Development of the Colle-Salvetti correlation-energy formula into a functional of the electron density. *Phys. Rev. B* **1988**, *37*, 785-789.
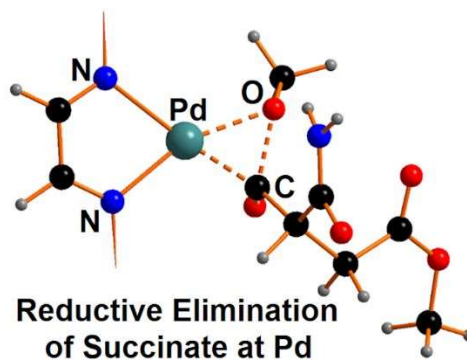
(17)   Mealli, C.; Proserpio, D. M. MO Theory Made Visible. *J. Chem. Educ.* **1990**, *67*, 399-402.

(18)   Although it cannot be excluded that the simplified N-N ligand underestimates the steric effects of the bulky aryl substituents at the N-N chelate, it is unlikely that the emerging mechanism pictures from the computations are dramatically altered.

(19)   (a) Barone, V.; Cossi, M. Quantum Calculation of Molecular Energies and Energy Gradients in Solution by a Conductor Solvent Model. *J. Phys. Chem. A* **1998**, *102*, 1995−2001. (b) Cossi, M.; Rega, N.; Scalmani, G.; Barone, V. Energies, structures, and electronic properties of molecules in solution with the C-PCM solvation model. *J. Comput. Chem.* **2003**, *24*, 669−681.

(20)   Golisz, S. R.; Hazari, N.; Labinger, J. A.; Bercaw, J. E. Activation of the C−N Bond in Nitromethane by Palladium α-Diimine Complexes. *J. Org. Chem.* **2009**, *74*, 8441-8443.

(21)   Dolg, M.; Wedig, U.; Stoll, H.; Preuss, H. Energy-adjusted Ab initio pseudopotentials for the first row transition elements. *J. Chem. Phys.* **86**, 866-872.

(22)   Milani, B.; Anzilutti, A.; Vicentini, L.; Sessanta o Santi, A.; Zangrando, E.; Geremia, S.; Mestroni, G. Bis-Chelated Palladium(II) Complexes with Nitrogen-Donor Chelating Ligands Are Efficient Catalyst Precursors for the CO/Styrene Copolymerization Reaction. *Organometallics* **1997,** *16,* 5064-5075.

(23)   In CO/alkene copolymerization reactions, olefins bearing EWGs have shown low coordination ability of the olefinic C=C on palladium species. For examples, see: (a) Philipp, D. M.; Muller, R. P.; Goddard, W. A.; Storer, J.; McAdon, M.; Mullins, M. Computational Insights on the Challenges for Polymerizing Polar Monomers. *J. Am. Chem. Soc.* **2002**, *124*, 10198-10210. (b) Boffa, L. S.; Novak, B. M. Copolymerization of Polar Monomers with Olefins Using Transition-Metal Complexes. *Chem. Rev.* **2000**, *100*, 1479-1493. (c) Mecking, S.; Johnson, L. K.; Wang, L.; Brookhart, M. Mechanistic Studies of the Palladium-Catalyzed Copolymerization of Ethylene and α-Olefins with Methyl Acrylate. *J. Am. Chem. Soc.* **1998**, *120*, 888-899.

(24)   Albright, T. A.; Burdett, J. K.; Whangbo, M.-H *"Orbital Interactions in Chemistry"* Second Edition John Wiley & Sons *inc*. 2014**.**

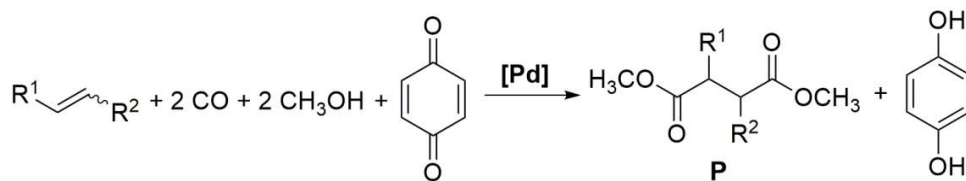(25)   Cambridge Structural Database System (CSD); Cambridge Crystallographic Data Centre: **2019**, Cambridge, U.K.

31

(26)   Forniés, J.; Martín, A.; Martín, L. F, Menjn, B.; Tsipis, A. All-Organometallic Analogues of Zeise's Salt for the Three Group 10 Metals. *Organometallics* **2005**, *24*, 3539-3546.

(27)   (a) Carfagna, C.; Gatti, G.; Mosca, L.; Paoli, P.; Guerri, A. Insertion Reactions of 1,2-Disubstituted Olefins with an *α*-Diimine Palladium(II) Complex. *Helv. Chim. Acta* **2006**, *89*, 1660-1671. (b) Carfagna, C.; Gatti, G.; Martini, D.; Pettinari, C. Syndiotactic CO/Styrene Copolymerization Catalyzed by α-Diimine Pd(II) Complexes: Regio- and Stereochemical Control. *Organometallics* **2001**, *20*, 2175-2182. (c) Carfagna, C.; Formica, M.; Gatti, G.; Musco A.; Pierleoni, A. Quantitative formation of the intermediate of alkene insertion in thecopolymerization of p-methylstyrene and carbon monoxide catalyzed by[(PriDAB)Pd(Me)(NCMe)]$^+$BAr$_4^-$. *Chem. Commun.* **1998**, 1113-1114.

(28)   For selected reviews, see: (a) Nozaki, K.; Hiyama, T. Stereoselective alternating copolymerization of carbon monoxide with alkenes. *J. Organomet. Chem.* **1999**, *576,* 248-253. (b) Bianchini, C.; Meli, A. Alternating copolymerization of carbon monoxide and olefins by single-site metal catalysis. *Coord. Chem. Rev.* **2002**, *225*, 35-66. (c) García Suárez, E. J.; Godard, C.; Ruiz, A.; Claver, C. Alternating and Non-Alternating Pd-Catalysed Co- and Terpolymerisation of Carbon Monoxide and Alkenes. *Eur. J. Inorg. Chem.* **2007**, 2582-2593. (d) Anselment, T. M. J.; Vagin, S. I.; Rieger, B. Activation of late transition metal catalysts for olefin polymerizations and olefin/CO copolymerizations. *Dalton Trans.* **2008**, 4537-4548.

(29)   Wu, F.; Foley, S. R.; Burns, C. T.; Jordan, R. F. Acrylonitrile Insertion Reactions of Cationic Palladium Alkyl Complexes. *J. Am. Chem. Soc.* **2005**, *127*, 1841-1853.

(30)   (a) Anderson, G. K.; Cross, R. J. Carbonyl-insertion reactions of square-planar complexes. *Acc. Chem. Res.* **1984**, *17*, 67–74. (b) Calderazzo, F. Synthetic and Mechanistic Aspects of Inorganic Insertion Reactions. Insertion of Carbon Monoxide. *Angew. Chem. Int. Ed.* **1977**, *16*, 299-311.

(31)   Duarte, F. J. S.; Poli, G.; Calhorda, M. J. Mechanistic Study of the Direct Intramolecular Allylic Amination Reaction Catalyzed by Palladium(II). *ACS Catal.* **2016**, *6*, 1772-1784.

(32)   (a) Catellani, M.; Mealli, C.; Motti, E.; Paoli, P.; Perez-Carreño, E.; Pregosin, P. S. Palladium−Arene Interactions in Catalytic Intermediates: An Experimental and Theoretical Investigation of the Soft Rearrangement between η^1 and η^2 Coordination Modes. *J. Am. Chem. Soc.* **2002**, 124, 4336-4346. (b) Càmpora, J.; Lopez, J. A.; Palma, P.; Valerla, P.; Spillner, E.; Carmona, E. Cleavage of

32

Palladium Metallacycles by Acids: A Probe for the Study of the Cyclometalation Reaction. *Angew. Chem., Int. Ed.* **1999**, *38*, 147-151. (c) Connelly, S. J.; Chanez, A. G.; Kaminsky, W.; Heinekey, D. M. Characterization of a Palladium Dihydrogen Complex. *Angew. Chem., Int. Ed.* **2015**, *54*, 5915-5918.

(33)   Vasseur, A.; Muzart, J.; Le Bras, J. Ubiquitous Benzoquinones, Multitalented Compounds for Palladium-Catalyzed Oxidative Reactions. *Eur. J. Org. Chem.* **2015**, 4053–4069.

(34)   The external H-bonding with acidic molecules is neglected for the sake of simplicity.

(35)   Hoffmann, R.; Alvarez, S.; Mealli, C.; Falceto, A.; Cahill, III, T. J.; Zeng, T.; Manca, G. From Widely Accepted Concepts in Coordination Chemistry to Inverted Ligand Fields. *Chem. Rev.* **2016**, *116*, 8173-8192.

(36)   (a) Walroth, R. C.; Lukens, J. T.; MacMillan, S. N.; Finkelstein, K. D.; Lancaster, K. M. Spectroscopic Evidence for a $3d^{10}$ Ground State Electronic Configuration and Ligand Field Inversion in $[Cu(CF_3)_4]^{1-}$. *J. Am. Chem. Soc* **2016**, *138*, 1922-1931. (b) DiMucci, I. M.; Lukens, J. T.; Chatterjee, S.; Carsch, K. M.; Titus, C. J.; Lee, S. J.; Nordlund, D.; Betley, T. A.; MacMillan, S. N.; Lancaster, K. M. Myth of d^8 Copper (III). *J. Am. Chem. Soc.* **2019**, *141*, 18508-18520.

(37)   Frisch, M. J.; Trucks, G. W.; Schlegel, H. B.; Scuseria, G. E.;Robb, M. A.; Cheeseman, J. R.; Scalmani, G.; Barone, V.; Mennucci,B.; Petersson, G. A.; Nakatsuji, H.; Caricato, M.; Li, X.; Hratchian, H.P.; Izmaylov, A. F.; Bloino, J.; Zheng, G.; Sonnenberg, J. L.; Hada, M.;Ehara, M.; Toyota, K.; Fukuda, R.; Hasegawa, J.; Ishida, M.; Nakajima,T.; Honda, Y.; Kitao, O.; Nakai, H.; Vreven, T.; Montgomery, J. A., Jr.;Peralta, J. E.; Ogliaro, F.; Bearpark, M.; Heyd, J. J.; Brothers, E.; Kudin,K. N.; Staroverov, V. N.; Kobayashi, R.; Normand, J.; Raghavachari, K.;Rendell, A.; Burant, J. C.; Iyengar, S. S.; Tomasi, J.; Cossi, M.; Rega,N.; Millam, J. M.; Klene, M.; Knox, J. E.; Cross, J. B.; Bakken, V.;Adamo, C.; Jaramillo, J.; Gomperts, R.; Stratmann, R. E.; Yazyev, O.;Austin, A. J.; Cammi, R.; Pomelli, C.; Ochterski, J. W.; Martin, R. L.;Morokuma, K.; Zakrzewski, V. G.; Voth, G. A.; Salvador, P.; Dannenberg, J. J.; Dapprich, S.; Daniels, A. D.; Farkas, O.; Foresman. J. B.; Ortiz, J. V.; Ciolowski, J.; Fox, D. J. Gaussian 0.9,revision B.01; Gaussian, Inc.: Wallingford, CT, 2010.

Table of Contents

**Reductive Elimination
of Succinate at Pd**

A detailed DFT study for a multi-step reaction, occurring at a square planar Pd(II) catalyst, describes the involvement of various reactants to give the main succinate product *via* a reductive elimination at the metal. The restoration of the active Pd(II) catalyst is performed by the benzoquinone (BQ) oxidant over a Pd(0) intermediate.

1
2
3
4
5
6
7
8
9
10
11
12
13
14
15
16
17
18
19
20
21
22
23
24
25
26
27
28
29
30
31
32
33
34
35
36
37
38
39
40
41
42
43
44
45
46
47
48
49
50
51
52
53
54
55
56
57
58
59
60

Scheme 1. Pd-catalyzed bis-alkoxycarbonylation reaction of alkenes involving carbon monoxide, methanol and p-benzoquinone.

134x25mm (300 x 300 DPI)
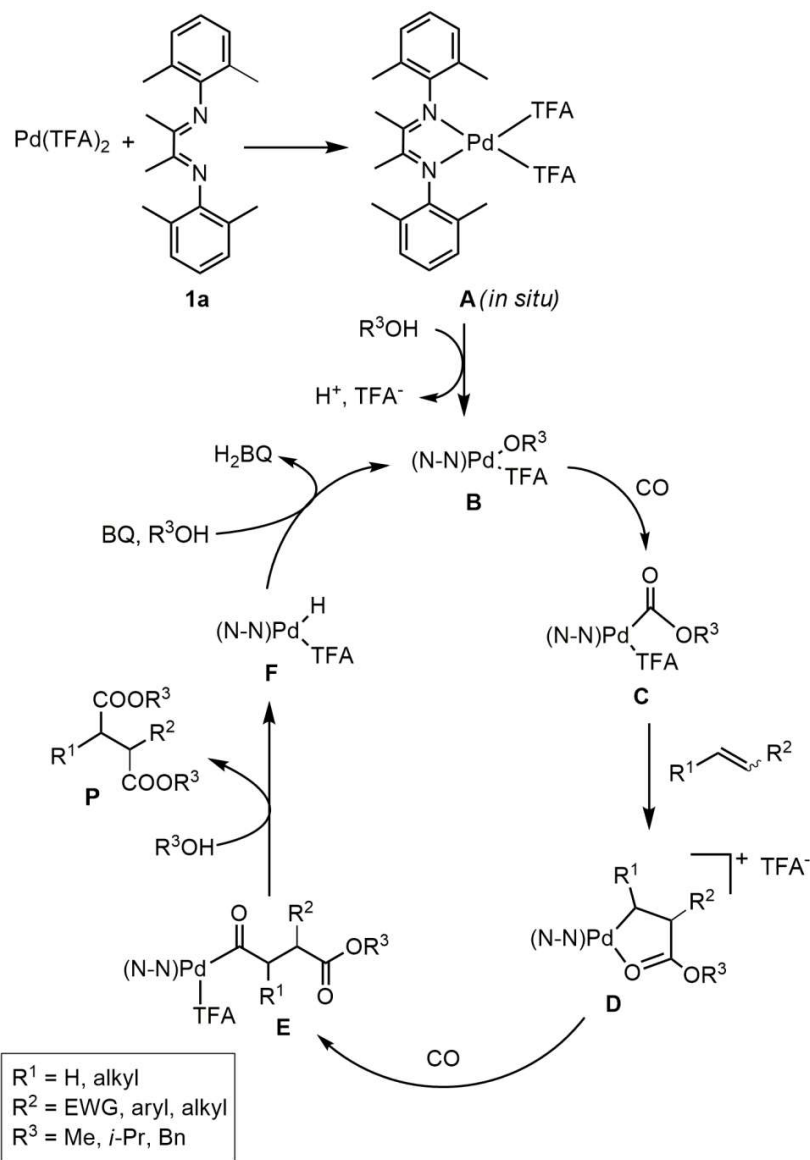
Scheme 2. Proposed catalytic mechanism for the bis-alkoxycarbonylation of olefins catalysed by aryl α-diimine/Pd(II) complexes. EWG = Electron-Withdrawing Group.

125x177mm (300 x 300 DPI)

1
2
3
4
5
6
7
8
9
10
11
12
13
14
15
16
17
18
19
20
21
22
23
24
25
26
27
28
29
30
31
32
33
34
35
36
37
38
39
40
41
42
43
44
45
46
47
48
49
50
51
52
53
54
55
56
57
58
59
60
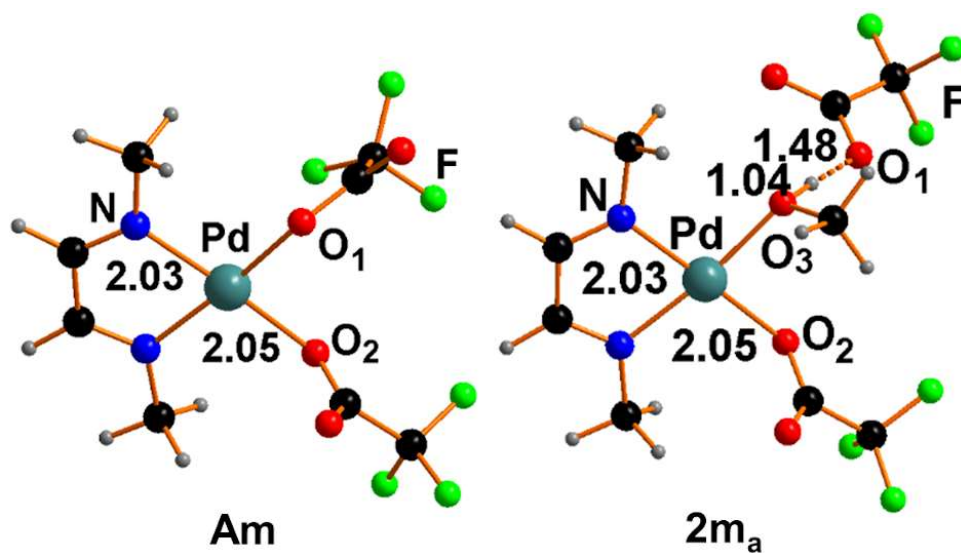
Figure 1. Optimized structures of the starting complex Am and the ion pair 2ma

80x45mm (300 x 300 DPI)
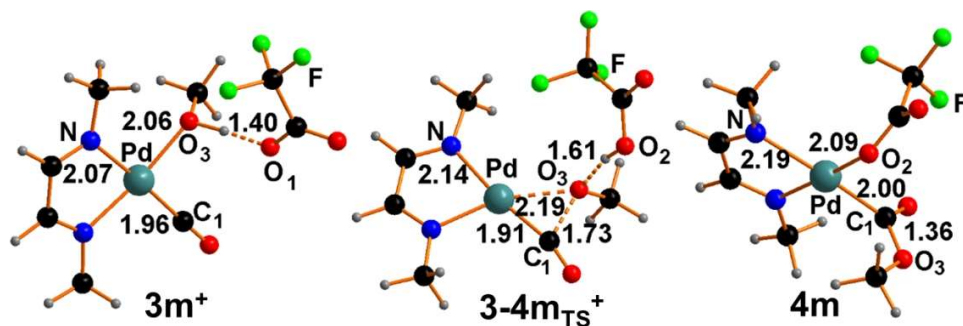
Figure 2. Cation 3m+ characterized by the CH3OH ligand H-bonded to TFA ; the transition state 3 4mTS+ for the methoxo/CO coupling, which, thanks to the H transfer, implies a momentarily formed HTFA unit; intermediate 4m with methoxycarbonyl and a TFA ligands.

113x37mm (300 x 300 DPI)
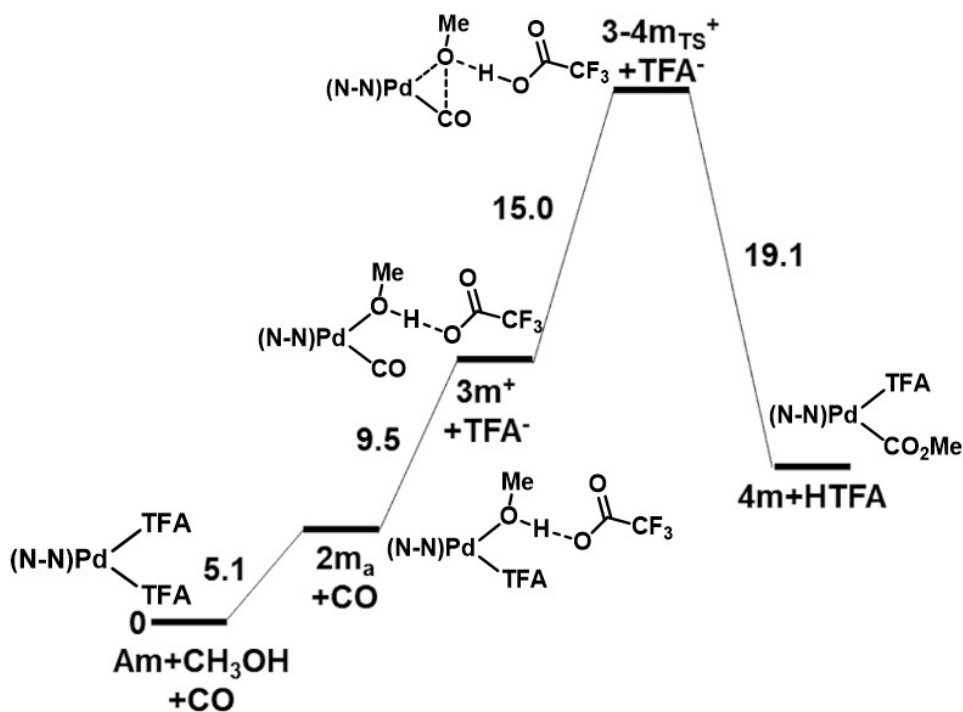
Figure 3. Free energy profile for the computed first part of the catalytic cycle corresponding to that in Scheme 2 (A→C or Am → 4m).
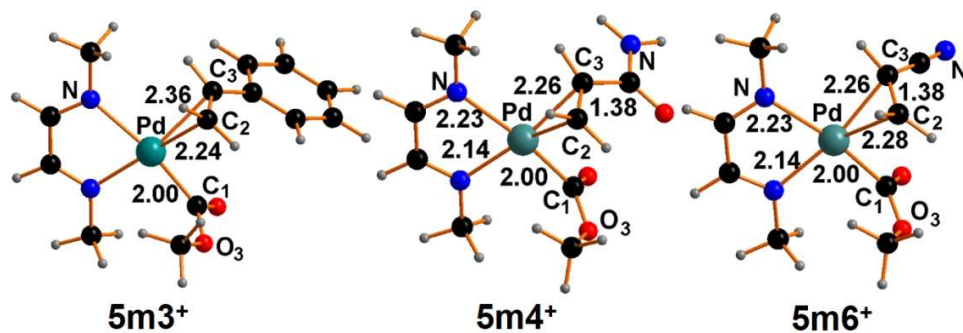
210x156mm (96 x 96 DPI)

Figure 4. Optimized structures of the three comparative η2-alkene complexes 5m3+ (styrene), 5m4+ (acryl amide) and 5m6+ (acrylonitrile).
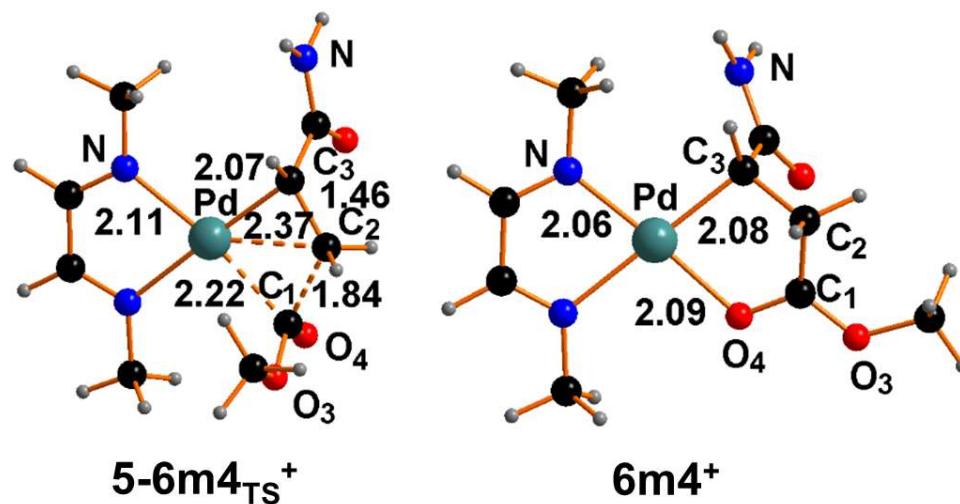
115x39mm (300 x 300 DPI)

Figure 5. Optimized structures of the transition state 5-6m4TS+ and the subsequent minimum 6m4+.
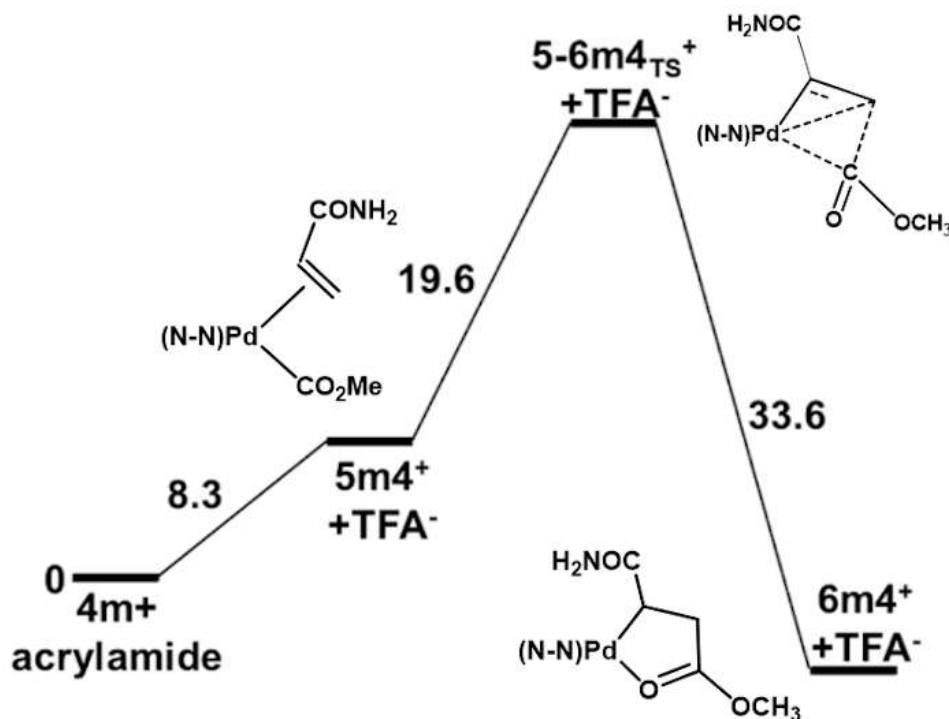
87x46mm (300 x 300 DPI)

Figure 6. Estimated free energy profile for the reaction of 4m+ with acrylamide to give the palladacycle 6m4+.

60x46mm (300 x 300 DPI)

1
2
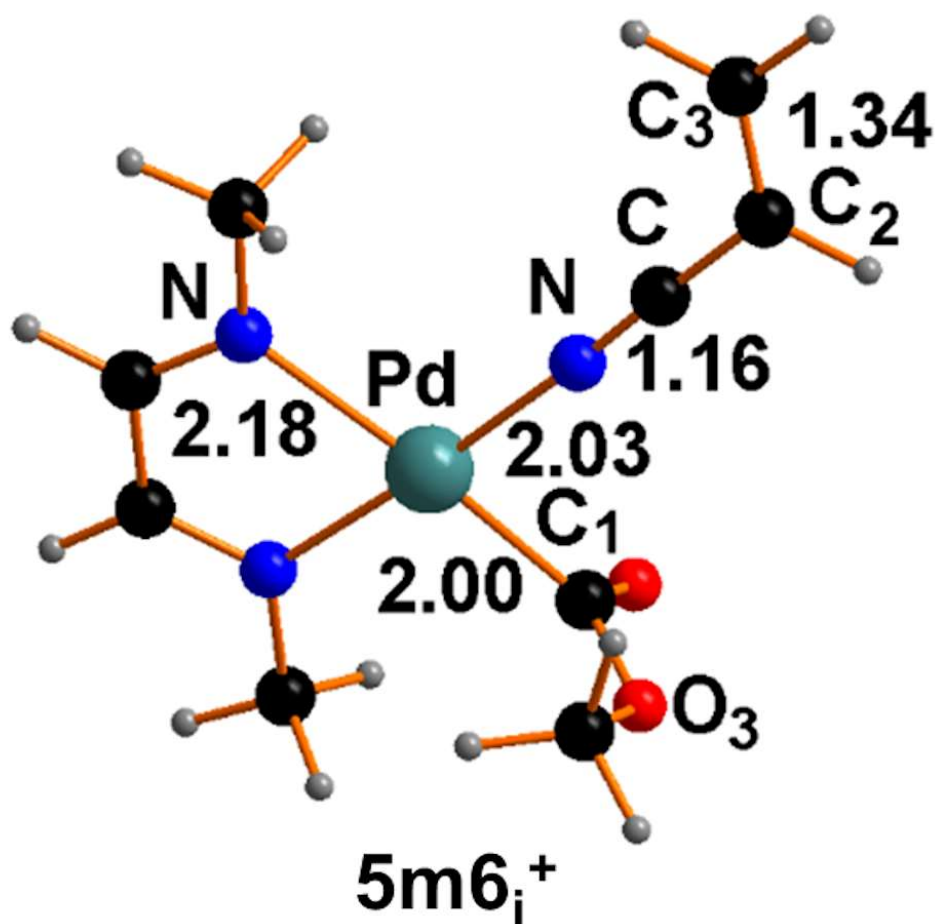3
4
5
6
7
8
9
10
11
12
13
14
15
16
17
18
19
20
21
22
23
24
25
26
27
28
29
30
31
32
33
34
35
36
37

Figure 7. Optimized coordination isomer 5m6i+ with the acrylonitrile ligand bound via the terminal N atom.

80x78mm (300 x 300 DPI)
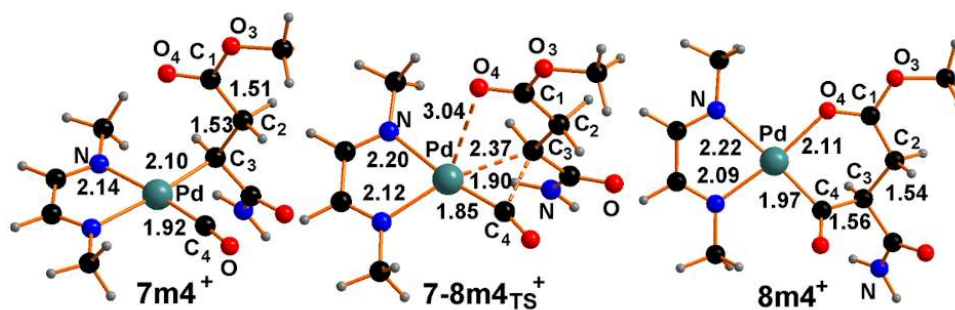
38
39
40
41
42
43
44
45
46
47
48
49
50
51
52
53
54
55
56
57
58
59
60

Figure 8. Optimized structures of 7m4+, the transition state for the alkyl-CO coupling 7 8m4TS+ and the subsequent intermediate 8m4+.

80x27mm (300 x 300 DPI)

1
2
3
4
5
6
7
8
9
10
11
12
13
14
15
16
17
18
19
20
21
22
23
24
25
26
27
28
29
30
31
32
33
34
35
36
37
38
39
40
41
42
43
44
45
46
47
48
49
50
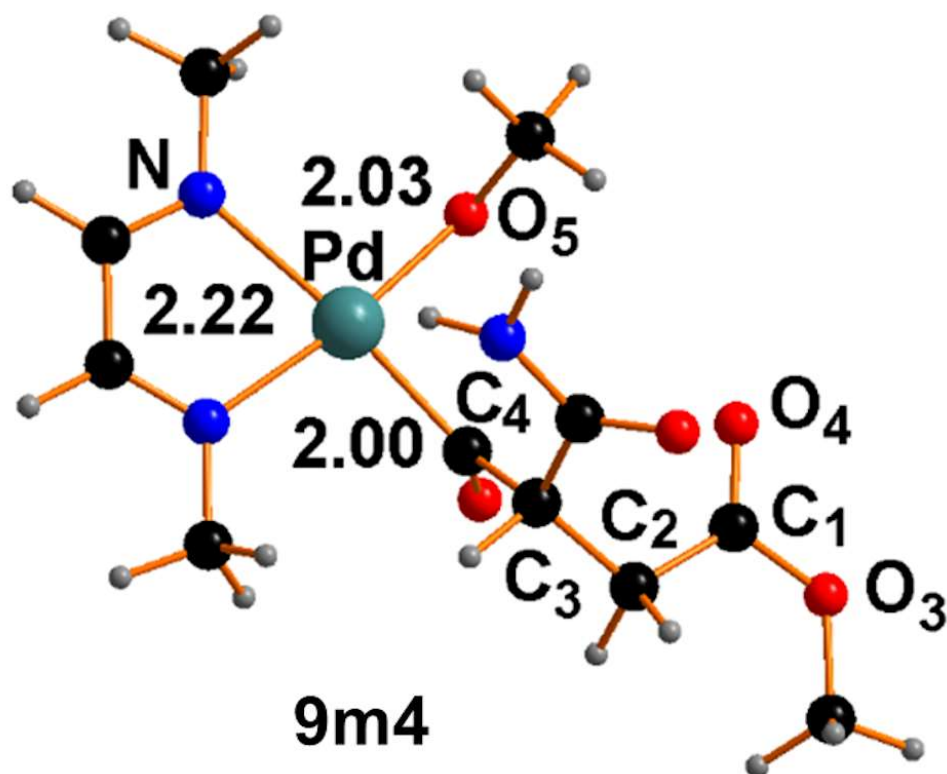51
52
53
54
55
56
57
58
59
60

Figure 9. Optimized structure of 9m4 as the immediate precursor of the main product P.
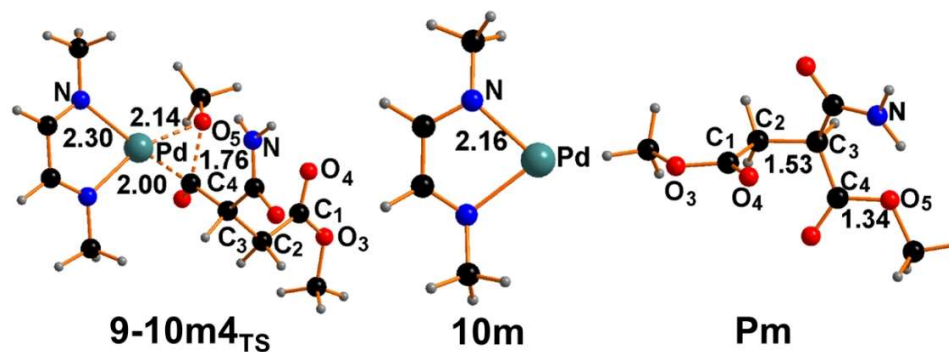
80x66mm (300 x 300 DPI)

Figure 10. Optimized structures 9-10m4TS, 10m and Pm proper of the reductive elimination process, which associates the formation of the succinate molecule with Pd(II)→Pd(0) reduction

105x39mm (300 x 300 DPI)

1
2
3
4
5
6
7
8
9
10
11
12
13
14
15
16
17
18
19
20
21
22
23
24
25
26
27
28
29
30

5-6m4$_{TS}^{+}$

19.6

33.6

7-8m4$_{TS}^{+}$

16.7

9-10m$_{TS}$

5m4^{+}
+ TFA^{-}

8.3

6.2

7.5

0

23.4

9m4
+HTFA

4m
+ olefin
(acrylamide)

2.1

7m4^{+}

12.5

Pm+10m
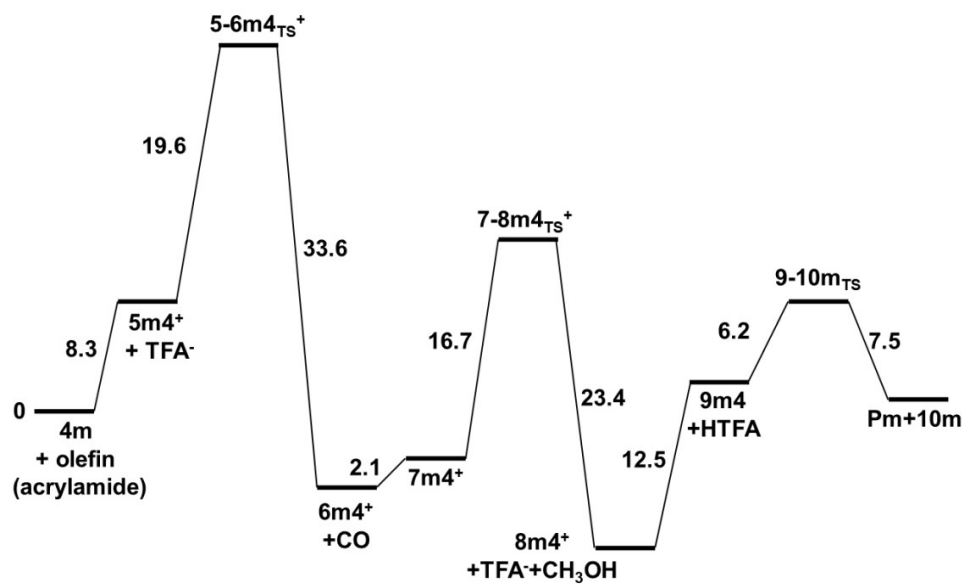
6m4^{+}
+CO

8m4^{+}
+TFA^{-}+CH$_3$OH

Figure 11. Summarized reaction profile for the portion of the cycle, which converts the alkoxycarbonyl/TFA complex 4m into the (N-N)Pd(0) species 10m together with di-ester product Pm.
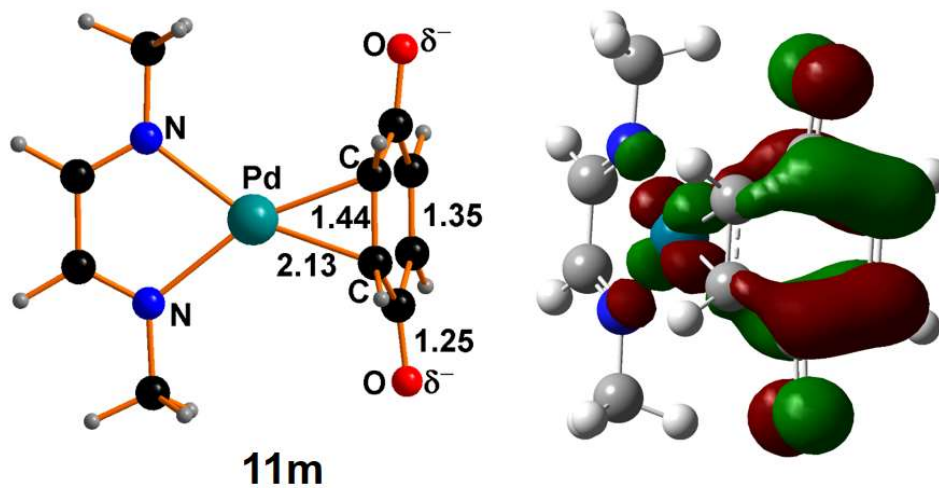
110x65mm (300 x 300 DPI)

31
32
33
34
35
36
37
38
39
40
41
42
43
44
45
46
47
48
49
50
51
52
53
54
55
56
57
58
59
60

Figure 12. Trigonal planar complex (N-N)Pd(η2-BQ), 11m; the vacant frontier antibonding MO formed by one Pd dπ orbital (populated) and a delocalized BQ pπ combination.

76x40mm (300 x 300 DPI)

1
2
3
4
5
6
7
8
9
10
11
12
13
14
15
16
17
18
19
20
21
22
23
24
25
26
27
28
29
30
31
32
33
34
35
36
37
38
39
40
41
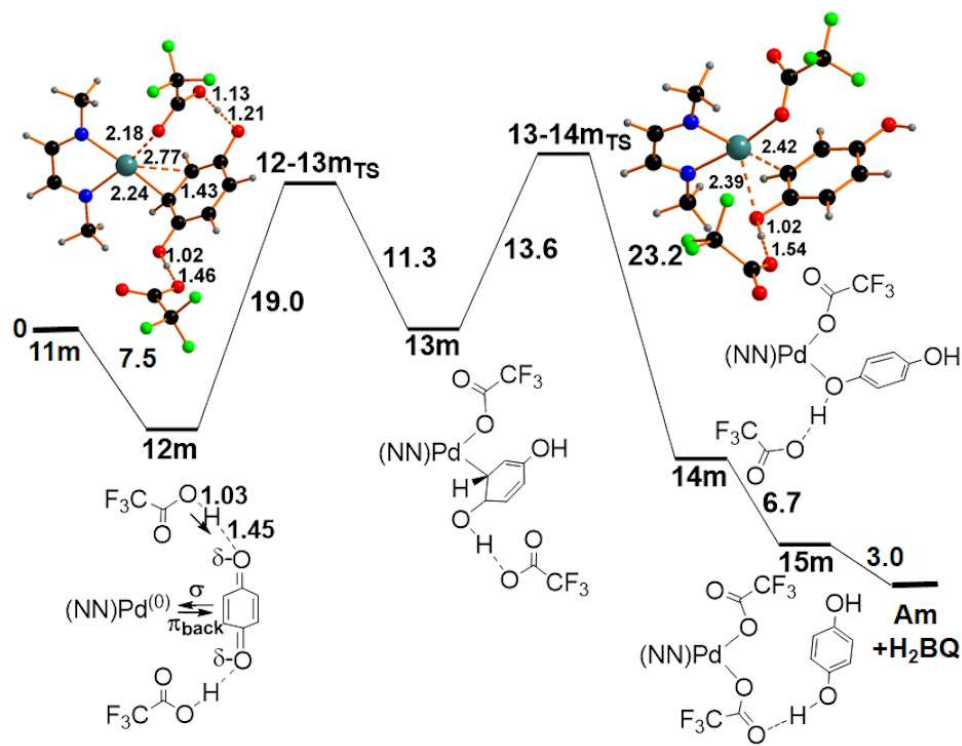42
43
44
45
46
47
48
49
50
51
52
53
54
55
56
57
58
59
60
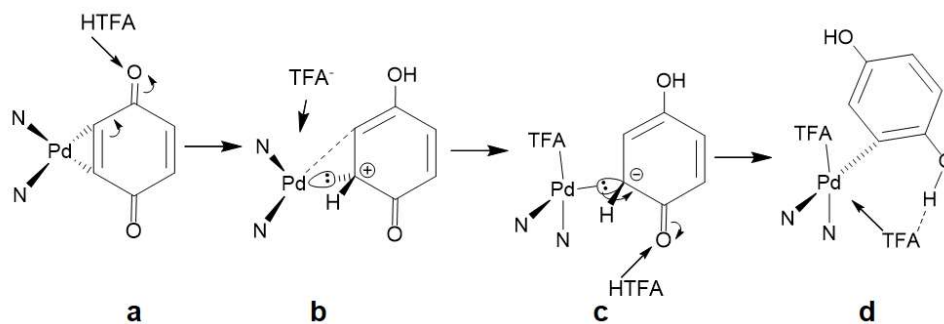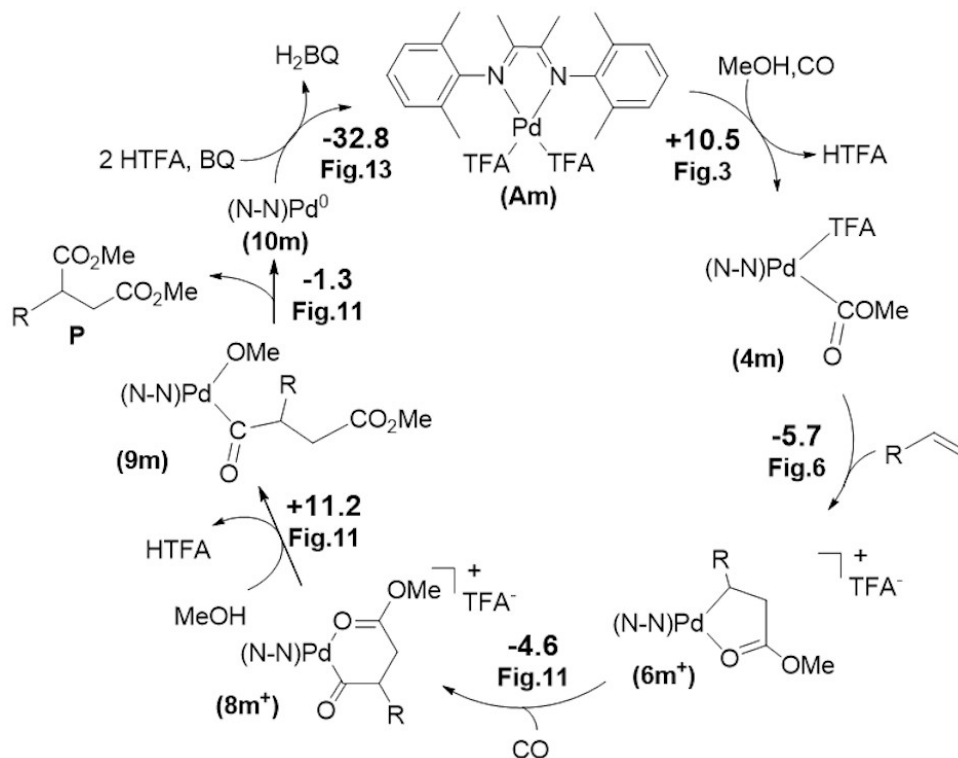

Figure 13. The Pd(0)→Pd(II) oxidation path, which, by involving the sacrificial BQ molecule, leads to the separated hydroquinone H2Q and the Am catalyst. All the schematized minima of the lower part of the figure are reported as ball and stick models in Figures S10-S13.

80x61mm (300 x 300 DPI)

Scheme 3. Qualitative description of the electron redistribution in going the Pd(0) complex 11m (a) to the Pd(II) adduct (N-N)Pd(II)TFA.H2BQ 15m (d).

84x28mm (300 x 300 DPI)

1
2
3
4
5
6
7
8
9
10
11
12
13
14
15
16
17
18
19
20
21
22
23
24
25
26
27
28
29
30
31
32
33
34
35
36
37
38
39
40
41
42
43
44
45
46
47
48
49
50
51
52
53
54
55
56
57
58
59
60

Scheme 4. Overall catalytic cycle for the bis-alkoxycarbonylation of mono-substituted olefins. The computed free energy balance in kcal·mol-1 is reported for any single step together with the Figure number presenting the corresponding detailed profile.

80x63mm (300 x 300 DPI)
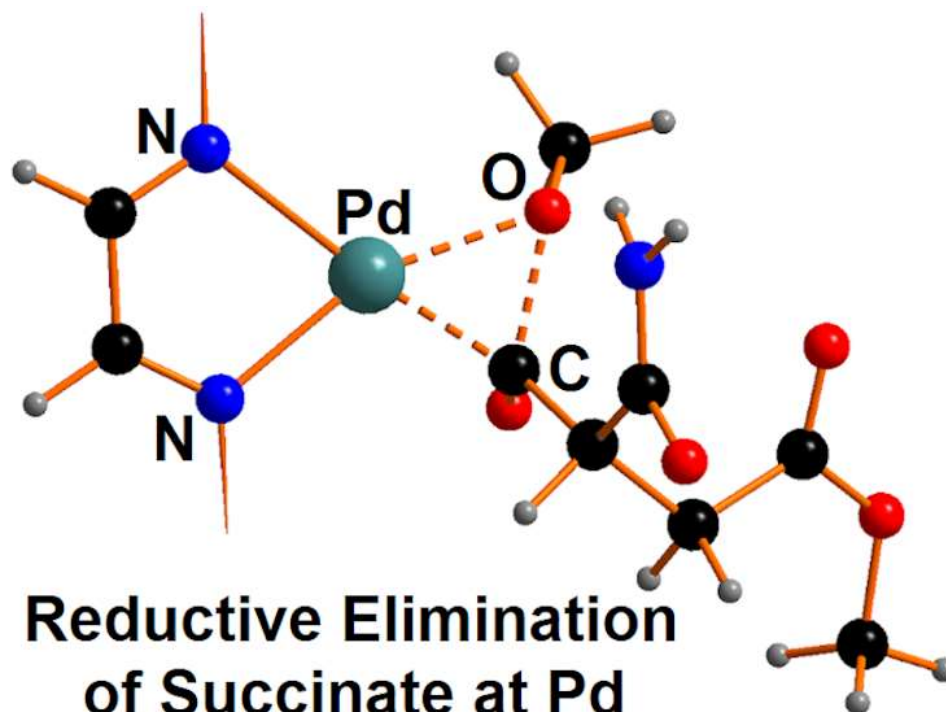
Reductive Elimination of Succinate at Pd

Table of content
Synopsis: A detailed DFT study for a multi-step reaction, occurring at a square planar Pd(II) catalyst, describes the involvement of various reactants to give the main succinate product via a reductive elimination at the metal. The restoration of the active Pd(II) catalyst is performed by the benzoquinone (BQ) oxidant over a Pd(0) intermediate.

63x47mm (300 x 300 DPI)